Journal of Sound and Vibration (2002) **255**(1), 1–41
doi:10.1006/jsvi.2000.3595, available online at http://www.idealibrary.com on IDEAL®

A SEMI-ANALYTICAL APPROACH TO THE NON-LINEAR DYNAMIC RESPONSE PROBLEM OF BEAMS AT LARGE VIBRATION AMPLITUDES, PART II: MULTIMODE APPROACH TO THE STEADY STATE FORCED PERIODIC RESPONSE

L. Azrar

Département de Mathématiques, Groupe de Modélisation Mathématique de Problèmes Mécaniques, Faculté, des Sciences et Techniques de Tanger, Université, Abdelmalek Essaadi, BP 416, *Tanger, Morocco*

R. Benamar

Laboratoire d'Etudes et de Recherches en Simulation, Instrumentation et Mesure, E.G.T. E.M.I., Université, Mohammed V, BP 765 *Agdal, Rabat, Morocco*

AND

R. G. White

*Department of Aeronautics and Astronautics, University of Southampton, Highfield, Southampton S*09 5*NH, England*

(*Received* 17 *December* 1999, *and in final form* 21 *December* 2000)

The semi-analytical approach to the non-linear dynamic response of beams based on multimode analysis has been presented in Part I of this series of papers (Azrar *et al*., 1999 *Journal of Sound and Vibration* **224**, 183–207 [1]). The mathematical formulation of the problem and single mode analysis have been studied. The objective of this paper is to take advantage of applying this semi-analytical approach to the large amplitude forced vibrations of beams. Various types of excitation forces such as harmonic distributed and concentrated loads are considered. The governing equation of motion is obtained and can be considered as a multi-dimensional form of the Duffing equation. Using the harmonic balance method, the equation of motion is converted into non-linear algebraic form. Techniques of solution based on iterative–incremental procedures are presented. The non-linear frequency and the non-linear modes are determined at large amplitudes of vibration. The basic function contribution coefficients to the displacement response for various beam boundary conditions are calculated. The percentage of participation for each mode in the response is presented in order to appraise the relation to higher modes contributing to the solution. Also, the percentage contributions of the higher modes to the bending moment near to the clamps are given, in order to determine accurately the error introduced in the non-linear bending stress estimated by different approximations. Solutions obtained in the jump phenomena region have been determined by a careful selection of the initial iteration at each frequency. The non-linear deflection shapes in various regions of the solution, the corresponding axial force ratios and the bending moments are presented in order to follow the behaviour of the beam at large vibration amplitudes. The numerical results obtained here for the non-linear forced response are compared with those from the linear theory, with available non-linear results, based on various approaches, and with the single mode analysis.

0022-460X/02/$35.00

1. INTRODUCTION

The use of beams and plates is extensive in various engineering structures and they are often subjected to dynamic loading. Dynamic loads are sometimes harmonic in nature or they may be idealized as harmonic excitations. The steady state response under these loads is of great importance in aerospace and mechanical engineering and other related fields. The study of the free and the forced vibration of geometrically non-linear beams involves obtaining solutions of the governing non-linear partial differential equations for which exact solutions are not available. Numerical methods are the only alternative for obtaining general solutions. Among the numerical methods available, the finite element method is undoubtedly the most versatile. The only problem with this method is that its formulation is quite laborious and it takes a large amount of computer storage. Despite the increase of computer capacities, direct integration of a set of non-linear equations representing a dynamic system often requires large computation time. Therefore, reduction techniques, assuming that the unknowns (the displacements for example) can be represented by a linear combination of several well-chosen functions, can be used. This permits considerable reduction of the number of non-linear equations to be solved and an economic solution with a reasonable accuracy. In linear vibration, the technique of modal analysis often represents an appropriate and an efficient procedure. The use of eigenmodes leads to a system of uncoupled differential equations that can be treated separately. For non-linear vibration, multimode analysis leads to a coupled non-linear system involving the contribution of various modes. Using the harmonic balance method, Benamar [2] and Benamar, Bennouna and White [3–7] reduced the non-linear free vibration problem to a set of non-linear algebraic equations. However, although the above model succeeded well in analyzing the effect of large vibration amplitudes on the mode shapes of beams, homogeneous and composite plates, it was restricted in a sense that only the free response problem was considered in the formulation. In Part I of the present work [1], a semi-analytical approach to the non-linear dynamic forced response problem was presented. Attention was particularly focused on the mathematical formulation and application of the model in a single mode analysis. The applicability of this method to the forced vibration of beams and some quantitative results was reported by Azrar and Benamar [8]. The objective here is the application of the non-linear forced vibration model previously reported using a multimode response approach to various types of excitation and boundary conditions, to present numerical results corresponding to each case, to examine how far they deviate from the linear theory and from the single mode approximation, and to discuss the range of validity of various assumptions.

In a survey of the literature on non-linear vibrations of beams, the most common methodological approaches are discussed. The assumption generally used is separation of time and space variables. Assuming that the non-linear deflection shape is proportional to the fundamental mode shape and using Galerkin's method, the governing dynamic equations can be reduced to a single non-linear ordinary differential equation in time of Duffing type. The latter equation may be treated by use of elliptical functions to obtain an exact mathematical solution, by perturbation methods or by the harmonic balance method to yield approximate solutions [1, 9–15]. A review of various formulations and assumptions made for large amplitude free vibration of beams has been given by Singh *et al.* [16]. Another approach generally used is to assume that the dependence in time is harmonic. Then, the harmonic balance method can be used to obtain a non-linear boundary value problem in the spatial variable. This technique is widely used because it permits transformation of the non-linear dynamic problem into a non-linear static one. This facilitates use of the same numerical methods as in static analysis.

A multiple-degree-of-freedom approach has been presented by Bennett and Esley [17]. Using three modes, the steady-state free and forced response and the stability of a beam with clamped ends at large vibration amplitudes have been investigated. A multimode analysis has been presented by Busby and Weingarter [18] using a finite element method and an averaging approach leading to an approximate solution to the non-linear equation under harmonic loading. This permitted the steady state response of beams using two modes to be studied. The experimental results presented in references [17, 18] confirm qualitatively the results of these analyses. In these two papers, the effectiveness of the multimode approach in non-linear vibrations of beams has been demonstrated. Using the Ritz method, an analytical solution for the non-linear free vibrations of beams has been given by Lewandowski [19]. The classical finite element method can be used to obtain an accurate solution of complex engineering problems. Most studies of non-linear vibrations of structures using this approach have been carried out by combining the finite element method and linearizing procedures [20–27]. Without linearizing functions, the problem of non-linear vibration of beams is solved by incremental–iterative methods [28–30]. An asymptotic numerical method for large amplitude vibrations has been developed by Azrar *et al.* [31, 32]. This method has been developed and applied to various non-linear structural problems by Potier-Ferry and co-workers. These studies have brought out the essential features which affect the practicability of the coupling of perturbation methods and finite element methods. A reduced basis technique has been presented by Noor *et al.* [33] for the non-linear vibration analysis of composite panels. The method of multiple scales, largely used by Nayfeh and co-workers, has been applied to obtain the non-linear modes of beams [34]. A finite element time domain modal formulation for large vibration amplitudes and non-linear random vibrations has been developed by Mei and co-workers. Applications of this method to free vibrations of beams and plates are presented by Shi, Lee and Mei [35, 36]. Theoretical and experimental investigations have been conducted by Bennouna and White [13] and Wolfe [37] in order to determine the effect of large vibration amplitudes on the fundamental mode of a clamped–clamped beam and the effect of non-linearity on the fatigue life of beam-like structures. Also, a careful investigation of the harmonic distortion spatial distribution induced by the geometrical non-linearity has been carried out. More recently, a comprehensive survey of the non-linear response of beams and plates at large amplitudes of vibration has been presented by Chen *et al.* [38]. A series of experimental investigations were conducted to understand the non-linear dynamic behaviour. A multimodal fatigue model was developed and applied to the test data with reasonable results. A comparison of finite element predicted non-linear beam random response with experimental results is presented in reference [38]. The aforementioned studies have contributed significantly to the understanding of the influence of geometrical non-linearities occurring at large vibration amplitudes of beams and plates. For deterministic forced vibration of beams, few studies have taken into account the effect of the coupling between higher modes in the non-linear range.

The present study focuses on non-linear forced vibrations of beams using a multimodal approach and taking into account the coupling between the higher vibration modes. The mathematical formulation for the dynamic response of beams leading to a multi-dimensional Duffing equation has been presented in reference [1] and is briefly reviewed here. The use of the harmonic balance method permitted conversion of the equation of motion into a non-linear algebraic model. Solution techniques based on continuation methods have been presented. Various types of excitations such as uniformly distributed and concentrated forces are considered. Numerical solution enabled the non-linear frequency response function to be derived, giving not only the displacement at the centre of the beam, as is usually the case, but the beam response spatial distribution

across the whole span, depending on the level of excitation, and involving distortion of the deflection shape, due to the non-linearity. Beams with various types of excitation and boundary conditions, such as simply supported–simply supported, simply supported–clamped and clamped–clamped have been considered. Numerical results are presented and compared with available results and with the single mode analysis. Multiple solutions corresponding to jump phenomena regions have been determined by a careful selection of the initial interaction at each frequency. The non-linear deflection shapes in various regions of the non-linear frequency response functions are presented for various types of excitation showing the amplitude dependence of the deflected shape of the beam. The axial force and the deflection moments are also presented for various amplitudes of vibration. The percentage participation of each mode is presented in order to appraise the relation to higher modes contributing to the solution. Also, the percentage contributions of the higher modes to the bending moment near to the clamps are given, in order to determine accurately the error introduced in the non-linear bending stress estimated via different approximations. The non-linear mode shapes in various regions of the solution, the axial force ratios and the moments are presented in order to follow the behaviour of the beam at large amplitudes. The numerical results obtained are compared with available results and with the single mode analysis.

2. REVIEW OF THE MATHEMATICAL FORMULATION

The problem of interest here is the non-linear forced vibration of beams. The non-linear effect, produced by large transverse vibration amplitudes, is axial stretching of the mid-plane of the beam. This effect is modelled by a non-linear strain–displacement relationship of the van Karman type. The basis of our considerations is the non-linear equation of motion obtained by a spatial discretization, in which the displacement function is expanded as a series on the linear beam mode shapes. This leads to a system of ordinary second order differential equations in the time domain involving the vector of the unknown modal contributions and can be considered as a multi-dimensional form of the Duffing equation. Assuming harmonic excitation, a non-linear algebraic model is obtained from the multi-dimensional Duffing equation using the harmonic balance method.

2.1. FORMULATION

In large amplitude vibrations of beams, the axial strain ε and the curvature K are defined as

$$\varepsilon = \frac{\partial U}{\partial x} + \frac{1}{2}\left(\frac{\partial W}{\partial x}\right)^2, \qquad K = \frac{\partial^2 W}{\partial x^2}, \tag{1}$$

where U and W are the axial and the transverse displacements respectively. The axial resultant force N and the bending moment M are related to ε and K, respectively, by

$$N = ES\varepsilon, \qquad M = EIK, \tag{2}$$

where E, S and I are Young's modulus, the area and the second moment of area of the cross-section of the beam. The elastic strain energy V of the beam is

$$V = \frac{1}{2}\int_0^L (N\varepsilon + MK)\,\mathrm{d}x. \tag{3}$$

For immovable beams, if one neglects the in-plane inertia, the non-linear stretching force N can be written in terms of transverse displacement, W, alone [1, 19, 24]. The total strain energy of the beam is given by the following formulation [1, 2]:

$$V = \frac{ES}{8L}\left[\int_0^L \left(\frac{\partial W}{\partial x}\right)^2 \mathrm{d}x\right]^2 + \frac{EI}{2}\int_0^L \left(\frac{\partial^2 W}{\partial x^2}\right)^2 \mathrm{d}x. \tag{4}$$

Neglecting the axial inertia, the kinetic energy is given by

$$T = \frac{1}{2}\rho S \int_0^L \left(\frac{\partial W}{\partial t}\right)^2 \mathrm{d}x. \tag{5}$$

The transverse displacement field, W, is assumed to have the form of the following series:

$$W(x, t) = \sum_{i=1}^{n} q_i(t) w_i(x), \tag{6}$$

in which $w_i(x)$ are the basic functions, chosen in the present work as the linear beam modes of vibration. The modal coefficients $q_i(t)$, are time-dependent generalized co-ordinates. Using these equations, discretization of the kinetic energy T and the total strain energy V leads to:

$$T = \tfrac{1}{2}\dot{q}_i \dot{q}_j m_{ij}, \tag{7a}$$

$$V = \tfrac{1}{2} q_i q_j k_{ij} + \tfrac{1}{2} q_i q_j q_k q_l b_{ijkl}, \tag{7b}$$

where the terms m_{ij}, k_{ij}, and b_{ijkl} are given as in references [1, 2, 5], by

$$m_{ij} = \rho S \int_0^L w_i(x) w_j(x)\, \mathrm{d}x, \tag{8a}$$

$$k_{ij} = EI \int_0^L \frac{\mathrm{d}^2 w_i}{\mathrm{d}x^2}\frac{\mathrm{d}^2 w_j}{\mathrm{d}x^2}\, \mathrm{d}x, \tag{8b}$$

$$b_{ijkl} = \frac{ES}{4L}\int_0^L \frac{\mathrm{d}w_i}{\mathrm{d}x}\frac{\mathrm{d}w_j}{\mathrm{d}x}\,\mathrm{d}x \int_0^L \frac{\mathrm{d}w_k}{\mathrm{d}x}\frac{\mathrm{d}w_l}{\mathrm{d}x}\,\mathrm{d}x. \tag{8c}$$

Assume that the structure is excited by a force $F(x, t)$ distributed over the range Ω (Ω is the length of the beam or a part of it). The physical force $F(x, t)$ excites the modes of the structures via a set of generalized forces $F_i(t)$ depending on the expression for F, the excitation point for concentrated forces, the excitation length for distributed forces, and the mode considered. The generalized forces $F_i(t)$ are given by

$$F_i(t) = \int_\Omega F(x, t) w_i(x)\, \mathrm{d}x, \tag{9}$$

in which $w_i(x)$ is the ith mode shape of the structure considered.

Using Lagrange's equation and the matrix formulation, the non-linear differential equation governing the dynamic behaviour of the forced beams is

$$\ddot{q}m_{ir} + q_i k_{ir} + 2q_i q_j q_k b_{ijkr} = F_r, \quad r = 1, n, \tag{10}$$

which can be written in a matrix form as

$$[\mathbf{M}]\{\ddot{\mathbf{q}}\} + [\mathbf{K}]\{\mathbf{q}\} + 2[\mathbf{B}(\mathbf{q})]\{\mathbf{q}\} = \{\mathbf{F}\}, \tag{11}$$

where $[\mathbf{M}]$, $[\mathbf{K}]$, $[\mathbf{B}]$, $\{\mathbf{q}\}$ and $\{\mathbf{F}\}$ are the mass matrix, the linear rigidity matrix, the non-linear rigidity tensor, the vector of generalized parameters and the vector of generalized forces respectively. It should be noticed here that the basic functions chosen in this paper, which are the beam linear mode shapes, lead to diagonal mass and rigidity matrices, due to orthogonality. This equation appears as a generalization of the non-linear case of the forced response equation, which is very well known in linear modal analysis,

$$[\mathbf{M}]\{\ddot{\mathbf{q}}\} + [\mathbf{K}]\{\mathbf{q}\} = \{\mathbf{F}\} \tag{12}$$

to which the term $2[\mathbf{B}(q)]$ corresponding to the non-linear rigidity is added.

It appears that the model presented above and summarized in equation (11) can be considered as a multi-dimensional form of the Duffing equation very often encountered in the non-linear vibration analysis of structures. It is worth noting here that the theory presented in references [1, 2] provides a means for calculating the cubic non-linearity coefficient in the approximate one-dimensional Duffing equation (2) for beams with various boundary conditions. This could allow numerical solutions to be obtained for engineering purposes, which would be valid as far as the single mode assumption is valid.

2.1.1. *Harmonic excitation*

Due to the fundamental nature of harmonic excitation and because it has many practical and theoretical applications, it will be the subject of this paper. Consider a beam excited by a concentrated harmonic force F^c applied at the point x_0, and also the case of a beam excited by a distributed harmonic uniform force F^d. The forces F^c and F^d are given by

$$F^c(x, t) = F^c \delta(x - x_0)\cos(\omega t), \qquad F^d(x, t) = F^d \cos(\omega t), \tag{13a, b}$$

in which δ is the Dirac function. The corresponding generalized forced $F_i^c(t)$ and $F_i^d(t)$ for each case are given by

$$F_i^c(t) = F^c w_i(x_0)\cos(\omega t) = f_i^c \cos(\omega t), \tag{14a}$$

$$F_i^d(t) = F^d \cos(\omega t) \int_0^L w_i(x)\,\mathrm{d}x = f_i^d \cos(\omega t). \tag{14b}$$

The dynamic equation representing the forced vibration of beams is obtained by introducing the generalized forces (14) into equation (11). Numerical solution of this equation yields the steady state motion of beams for various excitations and boundary conditions.

2.2. REVIEW OF RESULTS USING THE SINGLE MODE APPROACH

The single mode assumption consists of neglecting all the co-ordinates except the single "resonant" co-ordinate. Thus, it reduces the multi-degree-of-freedom system to a single-degree-of-freedom model. This approach is very often used because it greatly simplifies the theory and especially because the error introduced in the non-linear frequency remains small [1]. Using this approach, the non-linear dynamic system governing the motion is transformed into a non-linear differential equation of the Duffing type. An approximate solution of the later equation is generally obtained by the use of the harmonic balance method, by perturbation methods or the direct numerical integration. An exact solution of this equation exists only in the free vibration case or when the excitation force has a specified form of an elliptic function [9]. The amplitude–frequency relationships have been presented in Part I, based on the exact solution of the above equation in the free vibration case and results obtained by these relationships have been compared with available results for the cases of S–S and C–C beams under various excitations [1]. In order to obtain more practical formulae, the solution has been expanded into a power series. This leads to a higher order polynomial representation of the frequency–amplitude relationship. As clearly presented in reference [1], increasing order of the series does not increase the validity of the solution because of the divergence beyond the radius of convergence. This showed that extreme care must be taken in choosing the polynomial approximation given by perturbation procedures. A mathematical technique based on Padé approximants has been proposed in order to increase the range of amplitudes in which power-series expansions can be used. Formulations of the frequency–amplitude relationships have been proposed for very large amplitudes of vibration.

3. PRESENT ANALYSIS BASED ON THE MULTIMODE MODEL

3.1. GENERAL FORMULATION

Previous studies concerned with beams and plates [2, 4, 37] have shown that harmonic distortion of the non-linear response of the structure excited harmonically occurs at large transverse vibration amplitudes. However, the separation of harmonics carried out in the above references on experimental measurements of the non-linear response at various points of the structure considered and various excitation levels have shown that the higher harmonic components remain very small, compared with the first-harmonic component of the response. On the other hand, the comparison made in Part I of this series of papers between the exact solution of the Duffing equation, obtained in terms of elliptical functions, and that based on the assumption of a harmonic response, showed a very good agreement in the non-linear frequency estimates for a large range of vibration amplitudes ([1], Figure 4). Based on these two observations, the non-linear frequency response function has been assumed in the present paper, which is mainly concerned with the amplitude dependence of the first-harmonic component spatial distribution, to be given by

$$q_i(t) = a_i \cos(\omega t) \quad \text{for } i = 1\text{–}n. \tag{15}$$

Introducing equation (15) into equation (11) and applying the harmonic balance method leads to [1]

$$([\mathbf{K}] - \omega^2[\mathbf{M}])\{\mathbf{A}\} + \tfrac{3}{2}[\mathbf{B}(\mathbf{A})]\{\mathbf{A}\} = \{\mathbf{F}\}, \tag{16}$$

$$\{\mathbf{A}\} = \{a_1, a_2, \ldots, a_n\}^t.$$

In order to obtain a non-dimensional formulation, the non-linear parameters have been defined as follows:

$$w_i(x) = Rw_i^*\left(\frac{x}{L}\right) = Rw_i^*(x^*), \quad x^* = \frac{x}{L}, \quad R^2 = I/S, \quad \omega^2/\omega^{*2} = EI/\rho SL^4, \tag{17}$$

$$k_{ij}/k_{ij}^* = EIR^2/L^3, \quad m_{ij}/m_{ij}^* = \rho SR^2 L, \quad b_{ijkl}/b_{ijkl}^* = EIR^2/L^3,$$

where k_{ij}^*, m_{ij}^*, b_{ijkl}^* and ω^* are the non-dimensional generalized parameters.

Note that in Part I [1], the deflection $w(x)$ was assumed to be $w(x) = hw^*(x^*)$ and in this paper it is chosen to be $w(x) = Rw^*(x^*)$ in which R is the radius of gyration. This assumption is preferred here because it permits comparison with previously published results without further manipulations. The modal functions $w_i^*(x^*)$ are given in Appendix A for each boundary condition case considered in this study. The dimensionless generalized forces f_i^{c*} and f_i^{d*} corresponding to the concentrated force at x_0 and the uniformly distributed force on the whole beam, respectively, are given by

$$f_i^{c*} = F^c \frac{L^3}{EIR} w_i^*(x_0^*) = Forc^C w_i^*(x_0^*), \tag{18a}$$

$$f_i^{d*} = F^d \frac{L^3}{EIR} \int_0^1 w_i^*(x^*)\,\mathrm{d}x^* = Forc^d \int_0^1 w_i^*(x^*)\,\mathrm{d}x^*. \tag{18b}$$

Using the notation defined in equations (17) and (18), equation (16) gives the following non-linear algebraic equation:

$$([\mathbf{K}^*] - \omega^{*2}[\mathbf{M}^*])\{\mathbf{A}\} + \tfrac{3}{2}[\mathbf{B}^*(\mathbf{A})]\{\mathbf{A}\} = \{\mathbf{f}^*\}. \tag{19}$$

Expression (19) is used below for numerical solutions of the non-linear dynamic response of beams under various boundary conditions.

The 1-D non-linear frequency response function (1-DNFRF) is given by [1]

$$\frac{\omega^{*2}}{\omega_L^{*2}} = 1 + \tfrac{3}{2}\frac{b_{1111}^*}{k_{11}^*} a_1^2 - \frac{1}{k_{11}^*}\frac{f_1^*}{a_1}, \tag{20}$$

in which $\omega_L^{*2} = k_{11}^*/m_{11}^*$. The dimensionless amplitude at the centre of the beam is given by

$$A = \frac{w(centre)}{R} = a_1 w_1^*(\tfrac{1}{2}).$$

Using these notations, the following (1-DNFRF) is obtained:

$$\frac{\omega^{*2}}{\omega_L^{*2}} = 1 + \tfrac{3}{2}\frac{b_{1111}^*}{k_{11}^*}\frac{A^2}{[w_1^*(\frac{1}{2})]^2} - \frac{F}{A}, \tag{21}$$

in which F is defined in the case of a uniformly distributed and a concentrated harmonic force by

$$F^d = Forc^d \frac{w_1^*(\frac{1}{2})}{k_{11}^*} \int_0^1 w_i^*(x^*)\,\mathrm{d}x^* F^c = Forc^C \frac{w_1^*(\frac{1}{2})}{k_{11}^*} w_1^*(x_0^*). \tag{22}$$

These formulations are developed and discussed in Part I [1] for

$$A = \frac{h}{R} a_1 w_1^*(\tfrac{1}{2}) = \sqrt{12} a_1 w_1^*(\tfrac{1}{2})$$

and reformulated here for $A = a_1 w_1^*(\frac{1}{2})$ in order to avoid any confusion.

3.1.1. *Numerical details: the continuation methods*

To solve the non-linear governing equation of motion, incremental–iterative methods are generally used. The non-linear response of structures can include limit points or bifurcation points. The classical Newton-type method fails in the vicinity of these critical points, which makes it impossible to trace the post-critical range of the solution. Analysis of the non-linear forced vibration of structures requires solution of the equation of motion for various values of parameters such as the frequency and the amplitude of the excitation. It is well known that structures with certain types of non-linearities, such as cubic stiffness, can exhibit multiple response behaviours in certain frequency ranges and the solutions represent limit points. This can produce the jump phenomenon which is very well known in non-linear forced vibration. Then, continuation methods have to be used to obtain the path beyond critical points. Some continuation methods are well established and developed and applied in structural engineering. The most popular are the load control, displacement control and arc length methods [39–46]. Since the arc-length methods originally proposed by Crisfield [43] are essential to follow the non-linear solution, a general form of these procedures and their applicability to the problem considered here will be discussed briefly. The governing equation of non-linear forced vibration of beams presented above is written as

$$\{\mathbf{G}(\mathbf{A}, \omega^{*2})\} = [\mathbf{K}^*] \cdot \{\mathbf{A}\} - \omega^{*2}[\mathbf{M}^*] \cdot \{\mathbf{A}\} + \tfrac{3}{2}[\mathbf{B}^*(\mathbf{A})]\{\mathbf{A}\} - \{\mathbf{f}^*\} = \{\mathbf{0}\}, \tag{23}$$

where $\mathbf{G}$ is the residual vector. This equation represents n relations between $(n+1)$ unknowns $(a_1, a_2, a_3, \ldots, a_n, \omega^{*2})$. In order to solve this problem, an extra equation, denoted by $g(\mathbf{A}, \omega^{*2}) = 0$, can be introduced to complete the system. A numerical solution of the following extended system based on the Newtonian algorithm has to be carried out as follows:

$$\{\mathbf{G}(\mathbf{A}, \omega^{*2})\} = \{\mathbf{0}\}, \quad \{g(\mathbf{A}, \omega^{*2})\} = 0. \tag{24}$$

Iterative–incremental methods must be invariably used to solve the non-linear problem (24). The solution path is followed incrementally proceeding from a known solution $({}^1\mathbf{A}, {}^1\omega^{*2})$ to an adjacent configuration. Two strategies are usually followed to achieve equilibrium. The first, called prediction, is a procedure from a known configuration to the next; and the second, called correction, is an improvement of the predicted solution. These configurations presenting the prediction-correction solution are generally performed

following the Newton–Raphson procedure. This procedure is best introduced via a truncated Taylor series in a neighbourhood of the solution $({}^1\mathbf{A}, {}^1\omega^{*2})$ given by

$$\mathbf{G}({}^1\mathbf{A} + \Delta\mathbf{A}, {}^1\omega^{*2} + \Delta\omega^{*2}) = \mathbf{G}({}^1\mathbf{A}, {}^1\omega^{*2}) + \frac{\partial \mathbf{G}({}^1\mathbf{A}, {}^1\omega^{*2})}{\partial \mathbf{A}} \cdot \Delta\mathbf{A} + \frac{\partial \mathbf{G}({}^1\mathbf{A}, {}^1\omega^{*2})}{\partial \omega^{*2}} \Delta\omega^{*2} = 0, \tag{25}$$

where $\Delta\mathbf{A}$ and $\Delta\omega^{*2}$ are the increments. This can be written in a matrix form as

$$\mathbf{K}_t \cdot \Delta\mathbf{A} = -\mathbf{G}({}^1\mathbf{A}, {}^1\omega^{*2}) - \frac{\partial \mathbf{G}({}^1\mathbf{A}, {}^1\omega^{*2})}{\partial \omega^{*2}} \cdot \Delta\omega^{*2}, \tag{26}$$

where $\mathbf{K}_t$ is the tangent matrix of a configuration 1 given by $\mathbf{K}_t = \partial \mathbf{G}({}^1\mathbf{A}, {}^1\omega^{*2})/\partial \mathbf{A}$ Following equation (23), the derivatives in equation (25) are given by

$$\mathbf{K}_t = \mathbf{K}^* - {}^1\omega^{*2}\mathbf{M}^* + \tfrac{3}{2}[\mathbf{B}^*({}^1\mathbf{A}, {}^1\mathbf{A}, .) + \mathbf{B}^*({}^1\mathbf{A}, ., {}^1\mathbf{A}) + \mathbf{B}^*(., {}^1\mathbf{A}, {}^1\mathbf{A})],$$

$$\frac{\partial \mathbf{G}({}^1\mathbf{A}, {}^1\omega^{*2})}{\partial \omega^{*2}} = -\mathbf{M}^* \cdot {}^1\mathbf{A}, \tag{27}$$

where

$$B^*_{kl}({}^1\mathbf{A}, {}^1\mathbf{A}, .) = \sum_{i=1}^{n} \sum_{j=1}^{n} b^*_{ijkl} {}^1a_i {}^1a_j, \quad B^*_{jl}({}^1\mathbf{A}, ., {}^1\mathbf{A}) = \sum_{i=1}^{n} \sum_{k=1}^{n} b^*_{ijkl} {}^1a_i {}^1a_k,$$

and

$$B^*_{il}(., {}^1\mathbf{A}, {}^1\mathbf{A}) = \sum_{j=1}^{n} \sum_{k=1}^{n} b^*_{ijkl} {}^1a_j {}^1a_k.$$

The latter formulations can be simplified by using the symmetry of the tensor b^*_{ijkl}. Various strategies of resolution proposed in the literature for non-linear static and dynamic problems correspond to particular choices of equation $g(\mathbf{A}, \omega^{*2}) = 0$ [30, 40–49].

For the load control method, which is here termed frequency control, the additional constraint equation is $g(\mathbf{A}, \omega^{*2}) = \omega^{*2} - C = 0$, where C denotes a fixed frequency level. For displacement control, a value of one component of the vector $\mathbf{A}$ is specified; for example a_j, so that, $g(\mathbf{A}, \omega^{*2}) = a_j - \bar{a}_j$. The displacement component, which should be controlled is a_j and $\bar{a}_j$ is the value of the prescribed component of displacement. The frequency control method or the displacement control method fails when a frequency limit or a displacement limit exists. Using alternative increments of the amplitude of displacement or frequency, permits successful determination of backbone curves of a complex shape. This alternating method is presented in Appendix B and used here for computing the resonance curves. The shortcoming in the latter method is the necessity for modification of the tangential matrix during an iteration process.

Arc-length methods are intended to enable solution algorithms to pass limit points. For these methods, various formulations of the constraint equation $g(\mathbf{A}, \omega^{*2}) = 0$ are possible. The most popular methods keep a specific arc-length (s) constant, which is defined by Euclidean norm of the general displacement and frequency. The simplest formulation can

TABLE 1

Frequency ratios of free vibration and the modal participation of a C–C beam at various amplitudes. Case of three symmetric and three antisymmetric modes

Present analysis		Modal participation (%)			Shi and Mei [35]	Modal participation (%)		
w(centre)/R	ω^*/ω_L^*	a_1	a_3	a_5	ω^*/ω_L^*	a_1	a_3	a_5
1·00003	1·02220	99·8598	0·124537	0·156724E − 01	1·0221	99·84	0·15	1·5E − 2
1·50004	1·04922	99·6889	0·275959	0·351365E − 01	1·0484	99·61	0·34	4·3E − 2
2·00003	1·08578	99·4574	0·480423	0·621478E − 01	1·0854	99·59	0·33	7·9E − 2
2·50002	1·13086	99·1723	0·731219	0·964637E − 01	1·1339	99·17	0·59	0·25
3·00001	1·18336	98·8415	1·02075	0·137769	1·1842	98·66	1·17	0·16
3·50000	1·24224	98·4733	1·34102	0·185677	1·2439	98·12	1·5	0·30
4·00001	1·30652	98·0761	1·68416	0·239731	1·3020	98·00	1·66	0·34
4·50002	1·37537	97·6579	2·04270	0·299409	1·3721	97·73	1·87	0·40

be written as

$$g(\mathbf{A}, \omega^{*2}) = \|\Delta\mathbf{A}\|^2 + \alpha(\Delta\,\omega^{*2})^2 = s^2 = \text{constant}, \tag{28}$$

in which α is a scaling factor. The particular choice for the additional equation enjoys great popularity in view of the wide range of applications. They are, however, not always appropriate for all problems. The algorithms used for numerical results of this paper are presented in Appendix B.

4. NUMERICAL RESULTS AND DISCUSSIONS

The non-linear free and forced vibration analysis is obtained by numerical solution of equation (19). Various boundary conditions can be treated by a judicious choice of the modal functions. For the cases studied, the chosen functions are given in Appendix A. As far as the forcing is concerned, various types of excitation can be easily taken into account from equation (18).

4.1. FREE VIBRATION

4.1.1. *S–S beams*

In the case of free vibration of simply supported beams, there is no interaction between higher modes. This result is obtained by the algorithm presented here and also in previous works using multimodal analysis [17, 18]. The same conclusion was also reached by Mei *et al.* using a finite element time-modal formulation [35, 36]. Therefore, for a S–S beam, single mode analysis will yield an accurate estimate of fundamental frequency and the associated deformation shape.

4.1.2. *C–C beams*

For a clamped–clamped beam, there are interactions between various higher modes. In order to appraise these interactions, the modal participation of each mode may be given by

TABLE 2

Frequency ratios of free vibration and modal participation of a C–C beam at various amplitudes with six symmetric modes and comparison with the single mode analysis given by equation (21, $F = 0$)

Present analysis w(centre)/R	ω^*/ω_L^*	Modal participation (%)†						Single mode analysis equation (21, $F = 0$)
		a_1	a_3	a_5	a_7	a_9	a_{11}	
1·00000	1·02220	99·8545	0·124539	0·156749E − 01	0·363514E − 02	0·117244E − 02	0·464588E − 03	1·022231
1·50002	1·04922	99·6769	0·275996	0·351522E − 01	0·819018E − 02	0·264802E − 02	0·105081E − 02	1·049357
2·00002	1·08577	99·4360	0·480549	0·621992E − 01	0·145849E − 01	0·473135E − 02	0·188129E − 02	1·086196
2·50000	1·13084	99·1386	0·731523	0·965887E − 01	0·228311E − 01	0·743762E − 02	0·296475E − 02	1·131801
3·00002	1·18332	98·7926	1·02138	0·138029	0·329380E − 01	0·107838E − 01	0·431134E − 02	1·185159
3·50001	1·24216	98·4061	1·34213	0·186149	0·449047E − 01	0·147859E − 01	0·593146E − 02	1·245274
4·00001	1·30639	97·9875	1·68594	0·240519	0·587214E − 01	0·194588E − 01	0·783559E − 02	1·311218
4·50000	1·37515	97·5447	2·04540	0·300645	0·743632E − 01	0·248139E − 01	0·100333E − 01	1·382156
5·00002	1·44773	97·0850	2·41381	0·365982	0·917908E − 01	0·308588E − 01	0·125443E − 01	1·457359

†Participation of mode $i = 100a_i \Big/ \sum_{i=1}^{n} |a_i|$.

TABLE 3

Bending moments and modal contributions at various amplitudes of free vibration of a C–C beam

			Modal participation (%)†					
w(centre)/R	$M^*(0)$	$M^*(1/2)$	$a_1v_1^2$	$a_2v_2^2$	$a_3v_3^2$	$a_4v_4^2$	$a_5v_5^2$	$a_6v_6^2$
1·0001	28·501	−17·036	98·963	0·66708	0·20733	0·89408E − 01	0·46269E − 01	0·26718E − 01
1·5000	43·346	−25·387	97·71	1·4621	0·45983	0·19922	0·10335	0·59764E − 01
2·0000	58·892	−33·552	96·053	2·5085	0·80175	0·34959	0·18196	0·10543
2·5000	75·337	−41·483	94·046	3·7500	1·2227	0·53742	0·28090	0·16317
3·0000	92·863	−49·147	91·771	5·1272	1·7110	0·75923	0·39883	0·23235
3·5000	111·62	−56·520	89·306	6·5821	2·2543	1·0112	0·53424	0·31229
4·0000	131·74	−63·593	86·719	8·0631	2·8405	1·2895	0·68564	0·40230
4·5000	153·32	−70·362	84·072	9·5265	3·4577	1·5903	0·85146	0·50166
5·0000	176·44	−76·840	81·416	10·939	4·0955	1·9100	1·0303	0·60971
5·5000	201·17	−83·037	78·790	12·275	4·7440	2·2450	1·2206	0·72574
6·0000	227·53	−88·974	76·225	13·518	5·3947	2·5921	1·4210	0·84911
7·0000	285·26	−100·15	71·359	15·692	6·6756	3·3106	1·8471	1·1154
8·0000	349·62	−110·55	66·916	17·444	7·8936	4·0439	2·2985	1·4036
9·0000	420·47	−120·34	62·921	18·807	9·0213	4·7750	2·7665	1·7094
10·000	497·55	−129·63	59·361	19·834	10·044	5·4900	3·2431	2·0283

†Participation of the ith beam function to the curvature $= 100a_iv_i^2 \Big/ \sum_{i=1}^{n} |a_i|v_i^2$.

TABLE 4

Bending moments of free vibration of a C–C beam at various amplitudes with various modal analyses

	$M^*(0)$					
w(centre)/R	1-D	2-D	3-D	4-D	5-D	6-D
1·0004	28·218	28·408	28·457	28·483	28·496	28·504
1·5003	42·376	43·010	43·199	43·286	43·331	43·357
2·0004	56·605	58·083	58·514	58·737	58·829	58·891
2·5001	70·904	73·730	74·594	75·018	75·214	75·337
3·0003	85·315	90·079	91·547	92·291	92·646	92·862
3·5003	99·826	107·18	109·50	110·68	111·26	111·63
4·0002	114·45	125·07	128·52	130·31	131·20	131·74
4·5001	129·18	143·79	148·65	151·26	152·53	153·33
5·0003	144·05	163·34	169·96	173·57	175·34	176·45
5·5001	159·01	183·67	192·41	197·25	199·65	201·17
6·0000	174·08	204·78	215·99	222·38	225·52	227·53
6·5003	189·27	226·62	240·71	248·89	252·95	255·58
7·0003	204·54	249·12	266·47	276·76	281·93	285·28
7·5003	219·89	272·22	293·25	306·01	312·41	316·62
8·0000	235·32	295·86	320·99	336·56	344·42	349·62
8·5003	250·83	320·01	349·63	368·36	377·91	384·26
9·0000	266·38	344·55	379·10	401·39	412·82	420·47
9·5003	282·01	369·50	409·30	435·56	449·07	458·27
10·000	297·66	394·73	440·24	470·83	486·67	497·55

TABLE 5

Frequency ratios of free vibration of a C–C beam with various modal analyses

	ω/ω_L					
w(centre)/R	1-D	2-D	3-D	4-D	5-D	6-D
1·0000	1·0222308	1·0222	1·0222	1·0222	1·0222	1·0222
1·5000	1·0493572	1·0493	1·0492	1·0492	1·0492	1·0492
2·0000	1·0861967	1·0860	1·0858	1·0858	1·0858	1·0858
2·50000	1·1318012	1·1313	1·1309	1·1309	1·1308	1·1308
3·0000	1·1851592	1·1842	1·1834	1·1834	1·1833	1·1833
3·5000	1·2452746	1·2438	1·2422	1·2423	1·2421	1·2422
4·0000	1·3112182	1·3090	1·3065	1·3065	1·3064	1·3064
4·5000	1·3821561	1·3791	1·3754	1·3754	1·3751	1·3752
5·0000	1·4573591	1·4534	1·4481	1·4481	1·4477	1·4477
5·50000	1·5362010	1·5313	1·5240	1·5240	1·5234	1·5235

the following formulation, proposed by Mei *et al.* [35, 36]:

$$\text{participation of mode } i = 100a_i \Big/ \sum_{i=1}^{n} |a_i|. \tag{29}$$

This participation of each linear function to the first non-linear mode has been numerically computed and discussed for various cases. Results presented in Table 1 were obtained for

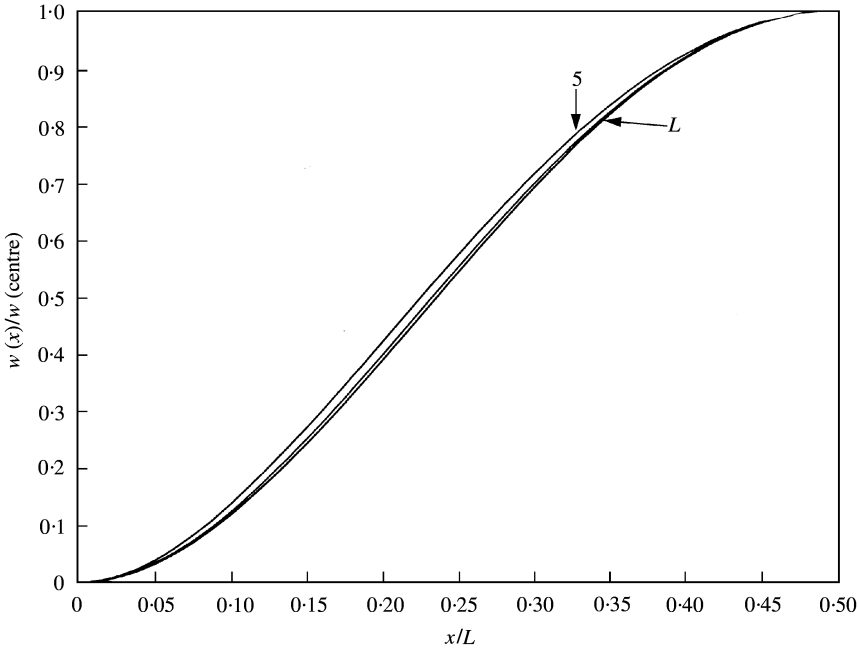

Figure 1. Linear and non-linear free vibration mode shapes of a fully clamped beam at amplitudes $W_{max}/R = 2{\cdot}5$ and $W_{max}/R = 5$.

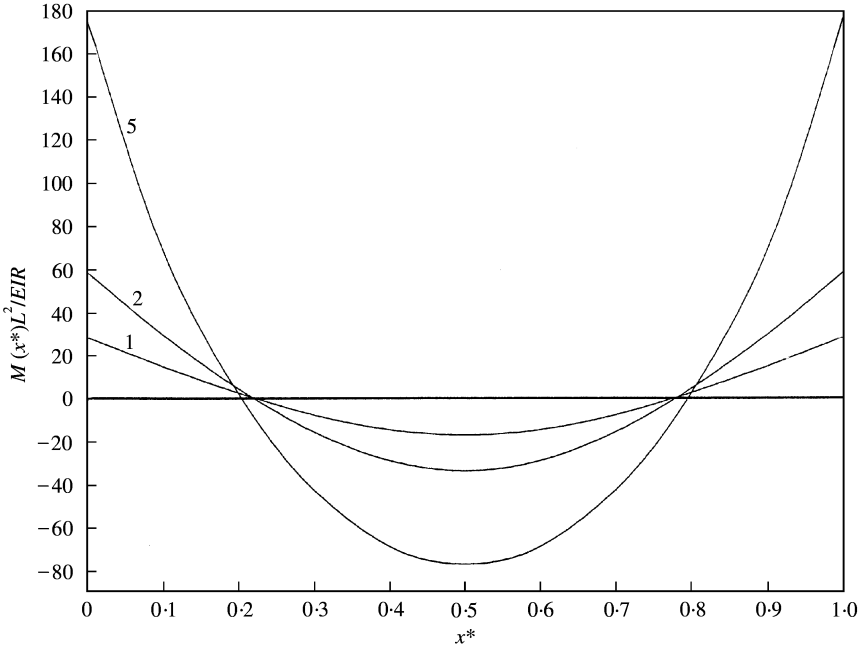

Figure 2. Non-linear free vibration bending moments of a fully clamped beam at amplitudes $W_{max}/R = 1$, 2 and 5.

TABLE 6

Frequency ratios of free vibration and modal participation of a clamped–simply supported beam at various amplitudes with six symmetric–antisymmetric modes

		Modal participation (%)†					
w(centre)/R	ω^*/ω_L^*	a_1	a_2	a_3	a_4	a_5	a_6
0·20000009	1·0020005	99·980065	0·15659098E − 01	0·29540117E − 02	0·86099379E − 03	0·32041186E − 03	0·14026947E − 03
0·40000008	1·0079712	99·920567	0·62359038E − 01	0·11791534E − 01	0·34405702E − 02	0·12811647E − 02	0·56108295E − 03
0·60000001	1·0178227	99·822406	0·13928189	0·26439774E − 01	0·77285770E − 02	0·28808099E − 02	0·12624503E − 02
0·80000001	1·0314123	99·687041	0·24510999	0·46779827E − 01	0·13708292E − 01	0·51169309E − 02	0·22443700E − 02
1·0000025	1·0485538	99·516409	0·37809095	0·72650404E − 01	0·21356797E − 01	0·79861737E − 02	0·35068184E − 02
1·5000019	1·1054561	98·951675	0·81483595	0·16012771	0·47574786E − 01	0·17897759E − 01	0·78890931E − 02
2·0000047	1·1793264	98·225099	1·3689008	0·27690899	0·83432634E − 01	0·31640582E − 01	0·14017824E − 01
2·5000027	1·2664137	97·382939	1·9996251	0·41830956	0·12816745	0·49079812E − 01	0·21878620E − 01
3·0000037	1·3635342	96·467971	2·6702803	0·57936731	0·18089441	0·70042332E − 01	0·31445107E − 01
3·5000039	1·4682112	95·515981	3·3511763	0·75520463	0·24064510	0·94317072E − 01	0·42675783E − 01
4·0000029	1·5786134	94·554767	4·0203797	0·94127884	0·30640363	0·12165791	0·55512529E − 01
4·5000026	1·6934189	93·604691	4·6629770	1·1335270	0·37713718	0·15178760	0·69880019E − 01
5·0000016	1·8116775	92·679911	5·2697421	1·3284349	0·45182275	0·18440293	0·85686027E − 01

†*Note*: See footnote to Table 2.

TABLE 7

Frequency vibration frequencies and axial force ratios for a clamped–simply supported beam at various amplitudes

	Present analysis		Sarma *et al.* [24]		Lewandowski [19]		Qaisi [15]
w(centre)/R	ω/ω_L	NL^2/EI	ω/ω_L	NL^2/EI	ω/ω_L	NL^2/EI	ω/ω_L
0·20000009	1·0020005	0·11027037	1·0026	0·1103	1·0020	0·1103	—
0·40000008	1·0079712	0·44080026	1·0106	0·4407	1·0300	0·4408	—
0·60000001	1·0178227	0·99076169	1·0237	0·9902	1·0178	0·9908	—
0·80000001	1·0314123	1·7588248	1·0416	1·7569	1·0314	1·7588	—
1·0000025	1·0485538	2·7432395	1·0641	2·7387	1·0486	2·7433	1·0841
1·5000019	1·1054561	6·1362812	1·1378	6·1167	1·1054	6·1365	1·1775
2·0000047	1·1793264	10·829791	1·2319	10·7771	1·1793	10·8303	1·2920
2·5000027	1·2664137	16·785058	1·3408	16·6787	1·2664	16·7863	1·4193
3·0000037	1·3635342	23·969218	1·4605	23·7907	1·3635	23·9716	1·5534
3·5000039	1·4682112	32·358081	1·5880	32·0941	1·4682	32·3620	1·6900
4·0000029	1·5786134	41·936638	1·7212	41·5779	1·5786	41·9428	1·8263
4·5000026	1·6934189	52·697774	1·8587	52·2454	1·6934	52·7063	1·9605
5·0000016	1·8116775	64·640254	1·9997	64·0989	1·8116	64·6515	2·0911

TABLE 8

Bending moments and modal contributions at various amplitudes of free vibration of a C–S beam

			Modal participation (%)†					
w(centre)/R	$M^*(0)$	$M^*(1/2)$	$a_1v_1^2$	$a_2v_2^2$	$a_3v_3^2$	$a_4v_4^2$	$a_5v_5^2$	$a_6v_6^2$
1·0000	21·794	−12·478	97·845	1·2047	0·48296	0·24278	0·13854	0·86214E − 01
1·5000	33·500	−18·710	95·386	2·5453	1·0436	0·53022	0·30438	0·19015
2·0000	46·101	−24·930	92·311	4·1689	1·7595	0·90655	0·52462	0·32940
2·5000	59·784	−31·128	88·864	5·9131	2·5809	1·3522	0·79017	0·49921
3·0000	74·680	−37·294	85·255	7·6474	3·4619	1·8484	1·0921	0·69487
3·5000	90·872	−43·421	81·641	9·2822	4·3644	2·3782	1·4223	0·91207
4·0000	108·40	−49·501	78·128	10·765	5·2586	2·9272	1·7736	1·1469
4·5000	127·27	−55·533	74·785	12·073	6·1231	3·4838	2·1396	1·3960
5·0000	147·49	−61·521	71·646	13·201	6·9434	4·0384	2·5151	1·6563
5·5000	169·01	−67·469	68·726	14·160	7·7103	4·5836	2·8954	1·9250
6·0000	191·79	−73·387	66·028	14·962	8·4192	5·1138	3·2767	2·1998
6·5000	215·80	−79·284	63·545	15·627	9·0685	5·6247	3·6557	2·4786
7·0000	240·96	−85·172	61·266	16·173	9·6587	6·1133	4·0296	2·7592
7·5000	267·21	−91·062	59·178	16·616	10·192	6·5776	4·3961	3·0400
8·0000	294·49	−96·964	57·265	16·973	10·672	7·0166	4·7534	3·3195
8·5000	322·72	−102·89	55·513	17·258	11·103	7·4298	5·1000	3·5962
9·0000	351·84	−108·85	53·908	17·483	11·488	7·8174	5·4350	3·8691
9·5000	381·79	−114·84	52·437	17·658	11·831	8·1799	5·7575	4·1372
10·000	412·49	−120·88	51·087	17·791	12·137	8·5181	6·0671	4·3996

†*Note*: See footnote to Table 3.

TABLE 9

Frequency ratios of free vibration of a C–S beam with various modal analyses

	ω/ω_L					
w(centre)/R	1-D	2-D	3-D	4-D	5-D	6-D
1·0001	1·0489	1·0485	1·0486	1·0486	1·0486	1·0485
1·5000	1·1069	1·1054	1·1055	1·1055	1·1055	1·1054
2·0000	1·1835	1·1792	1·1795	1·1795	1·1794	1·1793
2·5000	1·2751	1·2662	1·2669	1·2668	1·2665	1·2664
3·0000	1·3789	1·3631	1·3644	1·3643	1·3637	1·3635
3·5000	1·4923	1·4677	1·4697	1·4695	1·4685	1·4682
4·0000	1·6132	1·5781	1·5810	1·5806	1·5790	1·5786
4·5000	1·7401	1·6930	1·6970	1·6964	1·6940	1·6934
5·0000	1·8718	1·8115	1·8168	1·8159	1·8126	1·8117
5·5000	2·0074	1·9329	1·9397	1·9385	1·9340	1·9327
6·0000	2·1460	2·0567	2·0652	2·0636	2·0577	2·0560
6·5000	2·2872	2·1825	2·1930	2·1909	2·1834	2·1812
7·0000	2·4305	2·3101	2·3227	2·3201	2·3107	2·3079
7·5000	2·5756	2·4392	2·4541	2·4511	2·4395	2·4361
8·0000	2·7221	2·5696	2·5871	2·5835	2·5696	2·5654
8·5000	2·8698	2·7012	2·7213	2·7173	2·7008	2·6957
9·0000	3·0186	2·8338	2·8568	2·8522	2·8330	2·8269
9·5000	3·1684	2·9673	2·9934	2·9883	2·9660	2·9590
10·000	3·3189	3·1016	3·1309	3·1253	3·0999	3·0917

a C–C beam using the first six linear beam functions (three symmetric and three antisymmetric). These results are in good agreement with Shi and Mei's results. As may be expected, due to the symmetry of the first non-linear mode, it was found that the contributions of the antisymmetric beam functions are very small, compared with those of the symmetric functions which confirm results obtained previously [17, 18, 24]. Therefore, only the contributions of the symmetric beam functions have been given in Table 1. In Table 2, results obtained using six symmetric beam functions are presented, the contributions of each function and the corresponding non-linear frequency are given and compared with the single mode prediction. The contributions of higher modes appear to be relatively small. However, their effects on the curvatures, and hence on the non-linear bending moment estimates may not be negligible, since they intervene via their second derivatives, which involve multiplication by v_i^2, the v_i's being the beam parameters given in Appendix A. In order to examine the effect, another formula was used to estimate the percentage of participation of a given beam function, to the curvature, as follows:

$$\text{participation of the } i\text{th beam function to the curvature} = 100 a_i v_i^2 \Big/ \sum_{i=1}^{n} |a_i| v_i^2. \quad (30)$$

Percentages of the participation to the curvature of the first non-linear mode obtained using the new formula are summarized in Table 3. It can be seen that while the percentage of participation of the first beam function to the first non-linear mode given in Table 2 remains predominant and greater than 97·08% for values of the dimensionless amplitude w/R up to 5, its percentage of participation to the curvature is only 81·41% for $w(\text{centre})/R = 5$ and decreases to about 60% for $w/R = 10$, which correspond to $w(\text{centre})/h = 2{\cdot}887$. This

TABLE 10

Bending moments of free vibration of a C–S beam at various amplitudes with various modal analyses

	$M^*(0)$ and $M^*(1/2)$									
w(centre)/R	2-D		3-D		4-D		5-D		6-D	
1·0001	21·573	−12·529	21·693	−12·468	21·748	−12·455	21·776	−12·474	21·794	−12·478
1·5000	32·757	−18·876	33·157	−18·675	33·342	−18·630	33·438	−18·694	33·500	−18·710
2·0000	44·353	−25·311	45·287	−24·847	45·723	−24·740	45·951	−24·891	46·101	−24·930
2·5000	56·406	−31·841	58·193	−30·963	59·045	−30·757	59·489	−31·050	59·784	−31·128
3·0000	68·922	−38·469	71·936	−37·005	73·398	−36·653	74·166	−37·159	74·680	−37·294
3·5000	81·879	−45·191	86·527	−42·957	88·830	−42·402	90·047	−43·204	90·872	−43·421
4·0000	92·230	−51·995	101·94	−48·801	105·35	−47·985	107·16	−49·176	108·40	−49·501
4·5000	108·92	−58·870	118·14	−54·531	122·93	−53·383	125·50	−55·069	127·27	−55·533
5·0000	122·91	−65·808	135·06	−60·138	141·54	−58·588	145·03	−60·883	147·49	−61·521
5·5000	137·14	−72·795	152·64	−65·622	161·11	−63·596	165·73	−66·620	169·01	−67·469
6·0000	151·56	−79·825	170·80	−70·985	181·59	−68·406	187·53	−72·285	191·79	−73·387
6·5000	166·14	−86·887	189·47	−76·232	202·90	−73·026	210·36	−77·888	215·80	−79·284
7·0000	180·83	−93·974	208·59	−81·371	224·98	−77·463	234·18	−83·437	240·96	−85·172
7·5000	195·62	−101·08	228·10	−86·412	247·74	−81·729	258·89	−88·942	267·21	−91·062
8·0000	210·49	−108·20	247·92	−91·363	271·11	−85·833	284·43	−94·413	294·49	−96·964
8·5000	225·40	−115·33	268·03	−96·235	295·03	−89·794	310·74	−99·862	322·72	−102·89
9·0000	240·35	−122·47	288·35	−101·04	319·43	−93·624	337·73	−105·30	351·84	−108·85
9·5000	255·32	−129·62	308·87	−105·78	344·25	−97·336	365·34	−110·72	381·79	−114·84
10·0000	270·31	−136·77	329·53	−110·47	369·44	−100·94	393·51	−116·15	412·49	−120·88

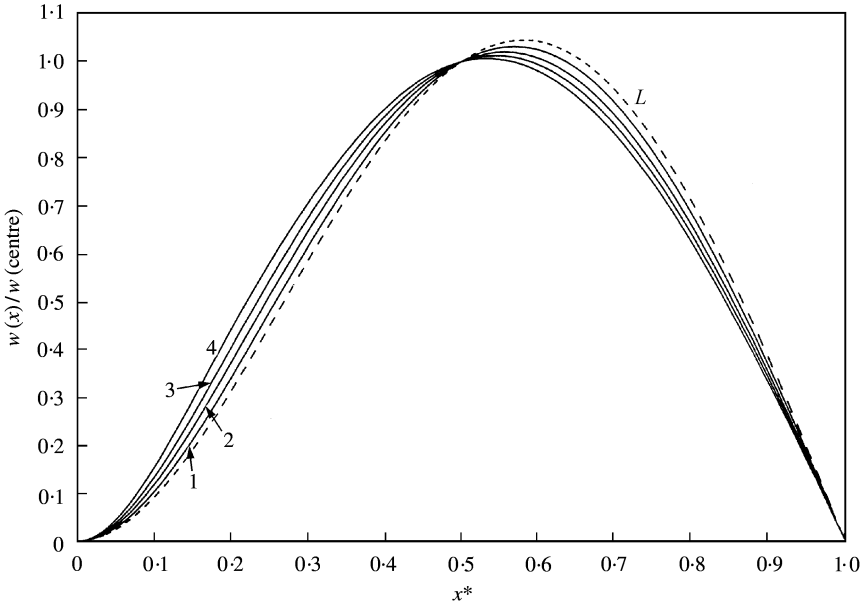

Figure 3. Linear and non-linear free vibration mode shapes of a clamped–simply supported beam at various amplitudes. *L*, linear mode; 1, 2, 3, 4, non-linear mode shapes at amplitudes $w(\text{centre})/R = 3$, 5, 7 and 10 respectively.

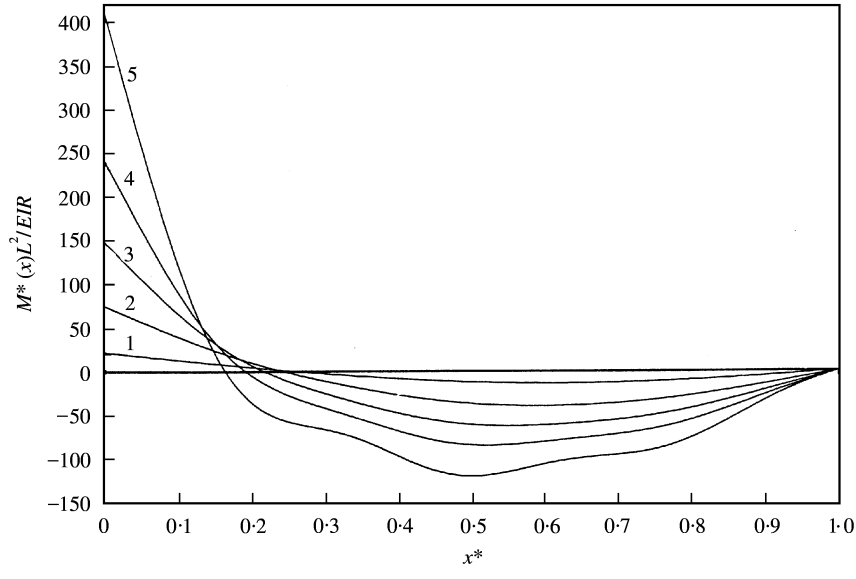

Figure 4. Non-linear free bending moments associated with the first non-linear mode shape of a clamped–simply supported beam at various amplitudes: 1, $w(\text{centre})/R = 1$; 2, $w(\text{centre})/R = 3$; 3, $w(\text{centre})/R = 5$; 4, $w(\text{centre})/R = 7$; 5, $w(\text{centre})/R = 10$.

shows that the influence of higher modes increases with the amplitude of vibration and that the consideration of the percentage of participation to the non-linear mode (i.e., equation (29)) may lead to inaccurate conclusions. Considering now the bending moment at the clamps, it appears from Table 4, in which results obtained using various approximations are

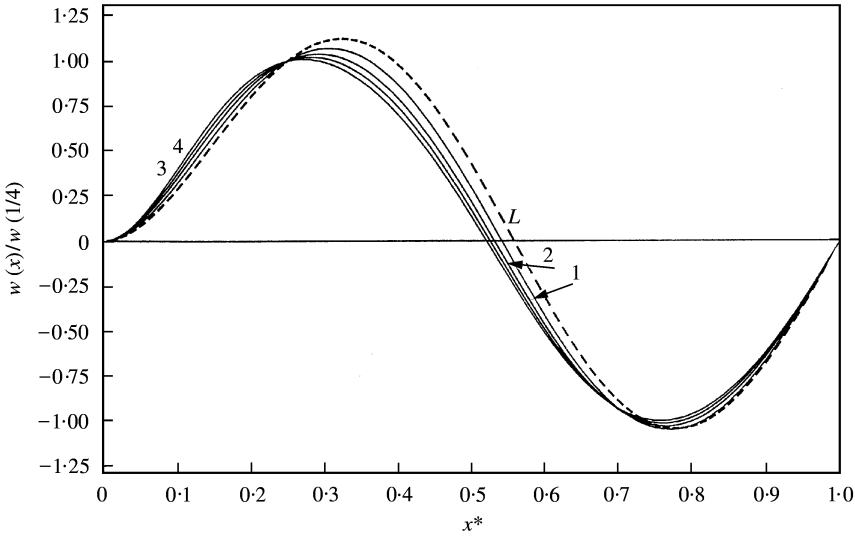

Figure 5. Linear and non-linear free vibration second mode shapes of a clamped–simply supported beam at various amplitudes. *L*, linear second mode; 1, 2, 3 and 4, non-linear second mode shapes at amplitudes $w(1/4)/R = 3$, 5, 7 and 10 respectively.

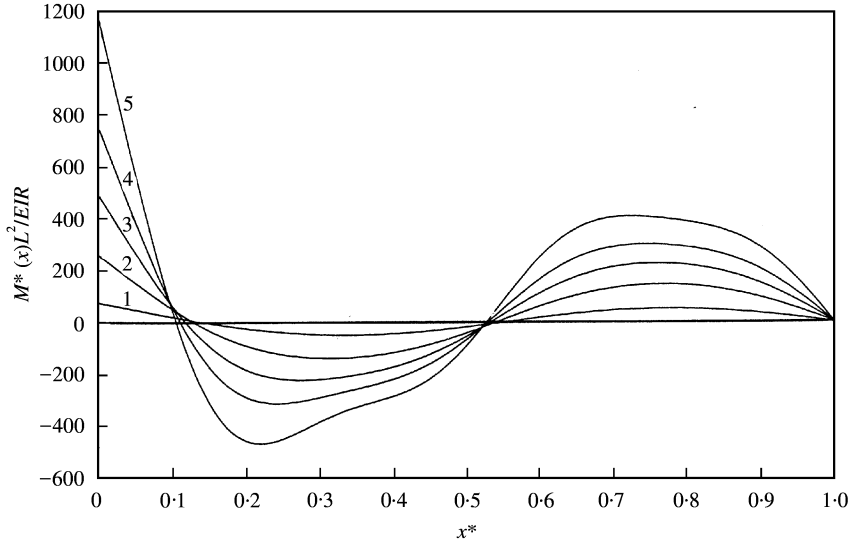

Figure 6. Non-linear free second bending moments associated with the second mode shape of a clamped–simply supported beam at various amplitudes 1, $w(1/4)/R = 1$; 2, $w(1/4)/R = 3$; 3, $w(1/4)/R = 5$; 4, $w(1/4)/R = 7$; 5, $w(1/4)/R = 10$.

listed, that the estimate of the non-dimensional bending moment at the clamps varies from a value of 297·66 using the single mode approach, to 497·54 obtained using six symmetric beam functions, which corresponds to a difference of about 40%. Also, the influence of the number of beam functions used in the non-linear frequency estimates has been considered. As may be seen from the numerical values listed in Table 5, it appears that, for a given amplitude of vibration, the non-linear frequency estimate decreases when the number of

TABLE 11

Frequency ratios of non-linear forced vibrations of a C–C beam under a harmonic concentrated force at the centre of the beam ($For^C = 200$). *Modal participation with six symmetric modes and comparison with the single mode analysis*

(For^C = 200.D0).		Modal participation (%)†						Single mode analysis (21)	
w(centre)/R	ω^*/ω_L^*	a_1	a_3	a_5	a_7	a_9	a_{11}	w(centre)/R	ω^*/ω_L^*
1·005353	0·1000000	96·39219	−2·874071	0·5100822	−0·1407441	0·5698181E − 01	−0·2593153E − 01	1·0	0·1928962
1·500927	0·6450033	97·75072	−1·740592	0·3633680	−0·8877219E − 01	0·3985901E − 01	−0·1668785E − 01	1·5	0·6552246
2·000284	0·8177417	98·57255	−1·020286	0·3050060	−0·5823117E − 01	0·3245784E − 01	−0·1146226E − 01	2·0	0·8221617
2·500852	0·9343069	99·19306	−0·4468246	0·2876531	−0·3529215E − 01	0·2944710E − 01	−0·7718413E − 02	2·5	0·9369499
3·000302	1·031101	99·58905	0·678134E − 01	0·2944021	−0·1518428E − 01	0·2897176E − 01	−0·4573171E − 02	3·0	1·033773
3·500347	1·120242	99·09354	0·5550099	0·3156096	0·4179276E − 02	0·3003896E − 01	−0·1619004E − 02	3·5	1·123735
4·000838	1·206412	98·56756	1·025542	0·3495403	0·2357336E − 01	0·3249186E − 01	0·1287302E − 02	4·0	1·211345
4·500776	1·291557	98·03852	1·483981	0·3935817	0·4354710E − 01	0·3610522E − 01	0·4260943E − 02	4·5	1·298619
5·000225	1·376679	97·51002	1·931526	0·4459033	0·6442957E − 01	0·4074151E − 01	0·7377538E − 02	5·0	1·386487
−5·000281	1·514947	−96·66279	−2·891753	−0·2879580	−0·1186933	−0·2120875E − 01	−0·1759812E − 01	−5·0	1·524941
−4·500031	1·453275	−97·05431	−2·601457	−0·2101410	−0·1045837	−0·1381919E − 01	−0·1568881E − 01	−4·5	1·460924
−4·000338	1·398263	−97·41199	−2·339205	−0·1347016	−0·9306238E − 01	−0·6814156E − 02	−0·1422664E − 01	−4·0	1·404005
−3·500208	1·351558	−97·72275	−2·118571	−0·608941E − 01	−0·8447389E − 01	−0·4549625E − 04	−0·1326006E − 01	−3·5	1·355963
−3·000673	1·315708	−97·92974	−1·958816	0·125113E − 01	−0·7936939E − 01	0·6690977E − 02	−0·1287480E − 01	−3·0	1·319287
−2·500924	1·294311	−97·91839	−1·887597	0·883801E − 01	−0·7863952E − 01	0·1377245E − 01	−0·1322210E − 01	−2·5	1·297718
−2·000244	1·293513	−97·74815	−1·958049	0·1729352	−0·8425936E − 01	0·2195301E − 01	−0·1464926E − 01	−2·0	1·297573
−1·499999	1·325402	−97·29274	−2·275527	0·2805047	−0·1004443	0·3287201E − 01	−0·1791381E − 01	−1·50	1·331533
−1·000629	1·420321	−96·20075	−3·130726	0·4529746	−0·1391726	0·5119060E − 01	−0·2518677E − 01	−1·0	1·432725
−0·8007563	1·494452	−95·35081	−3·817971	0·5680137	−0·1688901	0·6365799E − 01	−0·3065426E − 01	−0·80	1·512764
−0·6005462	1·612104	−93·94598	−4·968149	0·7461758	−0·2171378	0·8308178E − 01	−0·3946856E − 01	−0·60	1·641878
−0·4007967	1·819032	−91·26941	−7·185005	1·066063	−0·3059553	0·1179550	−0·5561330E − 01	−0·40	1·877914
−0·3009815	1·994473	−88·78509	−9·264190	1·347756	−0·3846030	0·1485001	−0·6986182E − 01	−0·30	2·088828
−0·2503182	2·119254	−86·89849	−10·85583	1·553040	−0·4418040	0·1706226	−0·8020222E − 01	−0·250	2·243612

†*Note*: See footnote to Table 2.

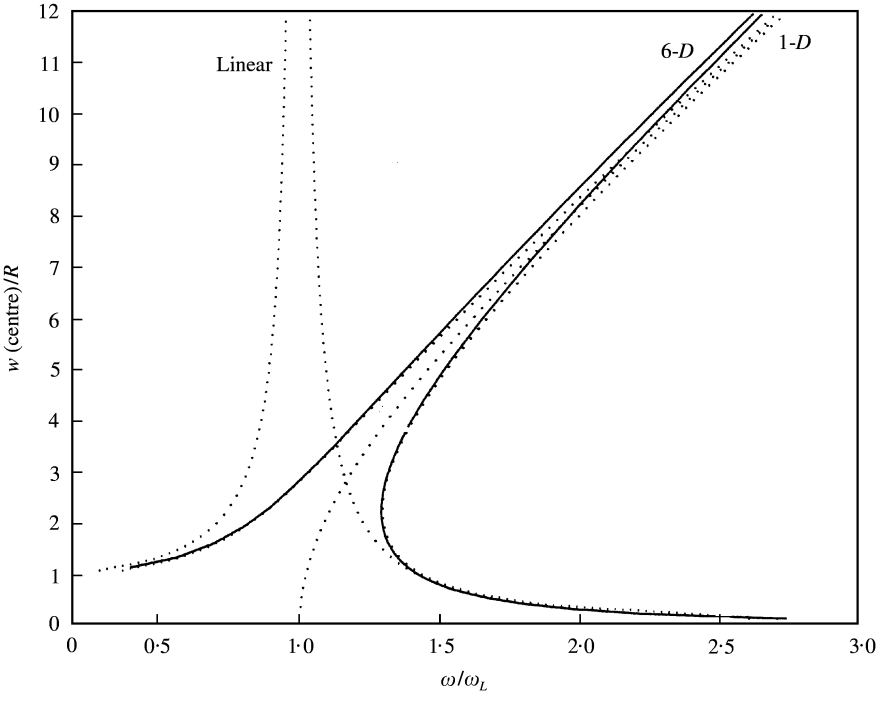

Figure 7. Resonance curves for forced vibrations of a C–C beam under a harmonic concentrated force at the centre of the beam ($For^C = 200$). Comparison with linear solution and non-linear solutions obtained by the single mode and the multimode approach.

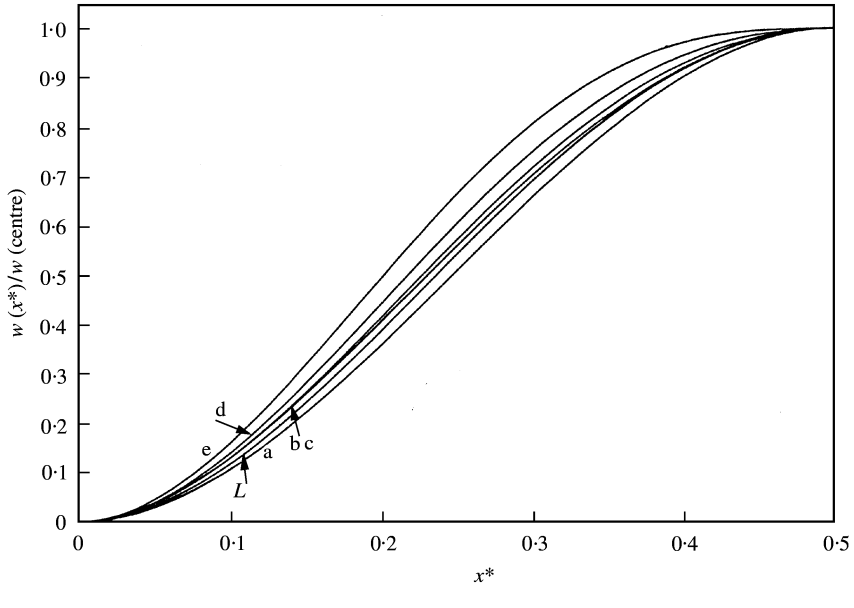

Figure 8. Linear and non-linear forced vibration mode shapes of a fully clamped beam under a harmonic concentrated force at the centre ($For^C = 200$) at various amplitudes. *L*, linear mode; a, b, c, d, e, non-linear mode corresponding to decreasing frequency from: a, ($\omega/\omega_L = 0{\cdot}5$, w(centre)$/R = 1{\cdot}2584$); b, ($\omega/\omega_L = 1{\cdot}2845$, w(centre)$/R = 4{\cdot}4594$); c, ($\omega/\omega_L = 1{\cdot}2884$, w(centre)$/R = -2{\cdot}2807$); d, ($\omega/\omega_L = 1{\cdot}7$, w(centre)$/R = -0{\cdot}5$); and e, ($\omega/\omega_L = 2$, w(centre)$/R = -0{\cdot}2984$).

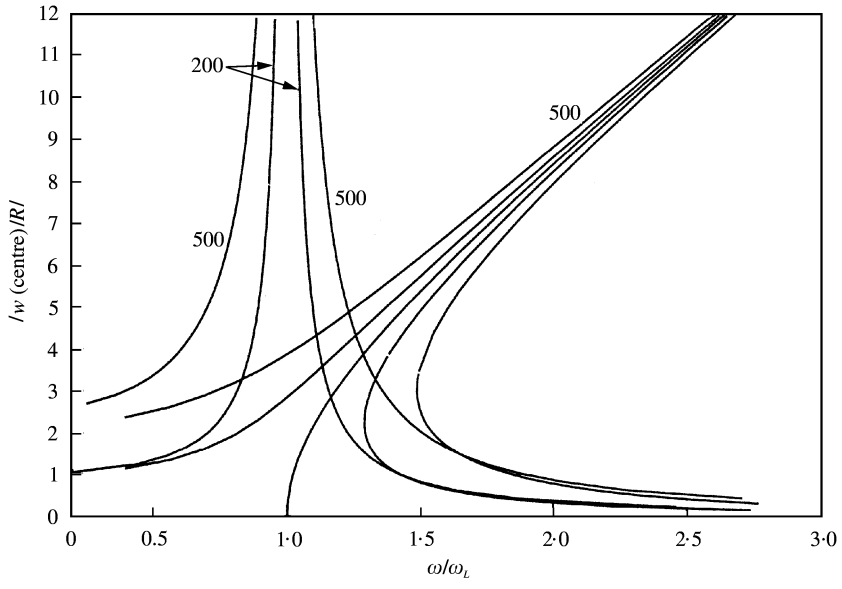

Figure 9. Linear and non-linear solutions of a C–C beam under a harmonic concentrated forces at the centre with the amplitudes $For^C = 200$ and 500.

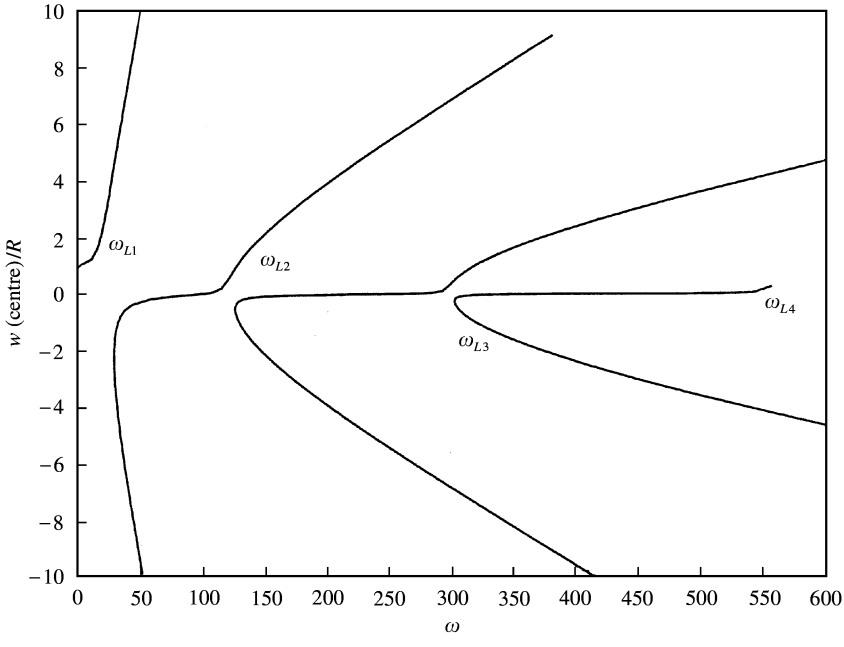

Figure 10. The first, second and third resonance curves of a C–C beam under a concentrated harmonic force at the centre ($For^C = 200$).

functions increases, which agrees well with the result usually expected in the Rayleigh–Ritz method, extended here to the non-linear case by use of Hamilton's principle. Also, the error introduced by the use of one beam function does not exceed 0·8% for $w/R = 5{\cdot}5$, which leads to the conclusion that a simple formula based on the single mode approach may be

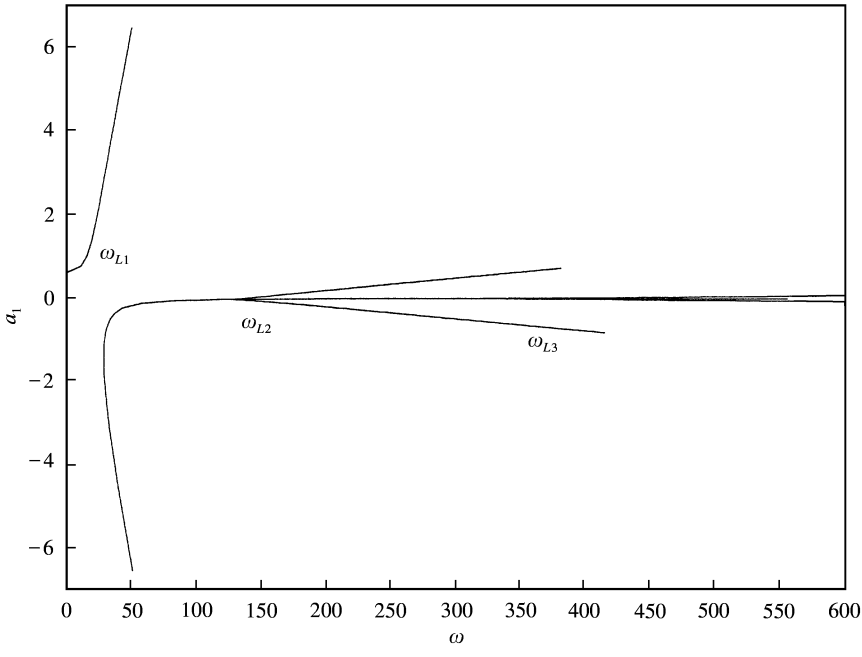

Figure 11. Contribution of a_1 on the first, second and third resonance curves of a C–C beam under a concentrated harmonic force at the centre ($For^C = 200$).

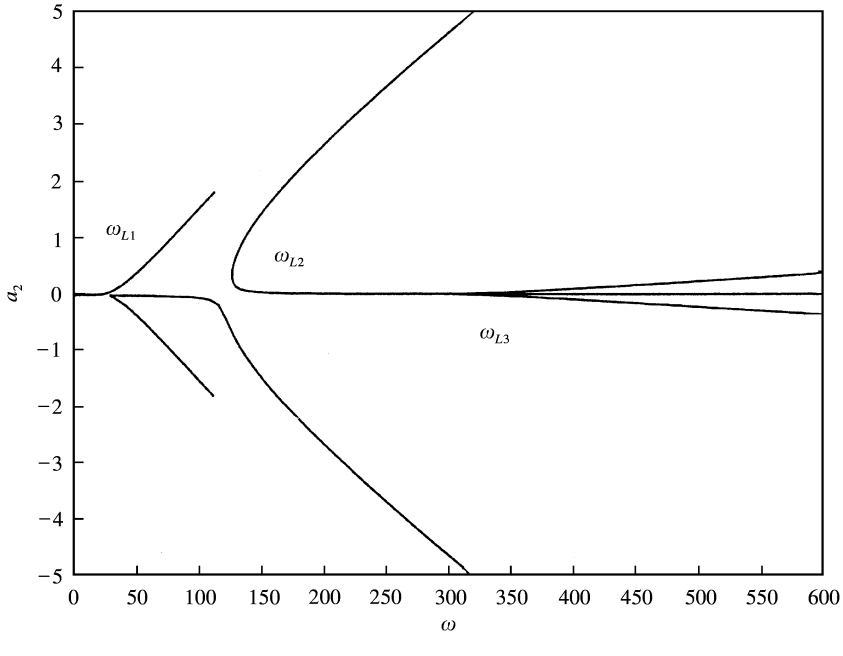

Figure 12. Contribution of a_2 on the first, second and third resonance curves of a C–C beam under a concentrated harmonic force at the centre ($For^C = 200$).

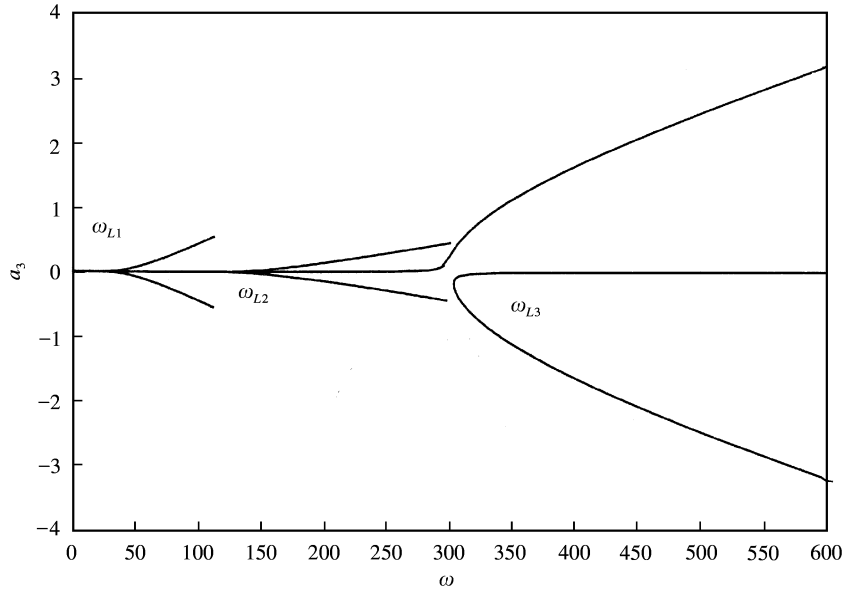

Figure 13. Contribution of a_3 on the first, second and third resonance curves of a C–C beam under a concentrated harmonic force at the centre ($For^C = 200$).

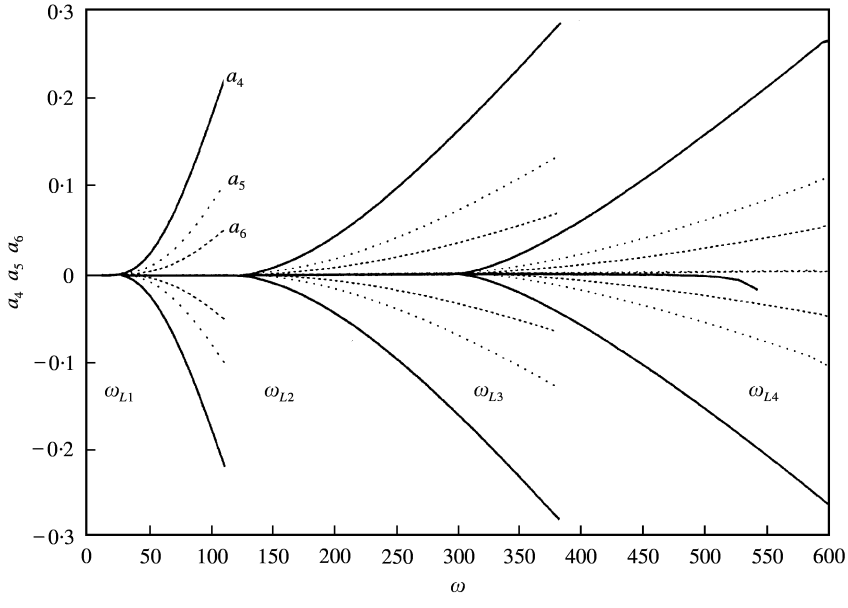

Figure 14. Contribution of a_4, a_5, a_6 on the first, second and third resonance curves of a C–C beam under a concentrated harmonic force at the centre ($For^C = 200$).

used for engineering purposes to estimate the non-linear frequency, while it may lead to inaccurate results when used to estimate the non-linear curvatures or bending moments, as explained above. The linear and the non-linear mode shapes at large amplitudes are presented in Figure 1. The bending moments associated with the free vibration of a C–C

TABLE 12

Frequency ratios of non-linear forced vibrations of a C–C beam at various amplitudes under a harmonic distributed force ($For^d = 1000$). *Modal participation with six symmetric modes and comparison with the single mode analysis*

(For^d = 1000.D0). 1000.D0). w(centre)/R	ω^*/ω_L^*	Modal participation (%)†						Single mode analysis (21) ω^*/ω_L^*
		a_1	a_3	a_5	a_7	a_9	a_{11}	
2.2500981	0·26900446	97·508930	2·1585640	0·25169864	0·56097928E − 01	0·17690445E − 01	0·70186805E − 02	0·23663252
2·5000771	0·48927845	97·548453	2·1173660	0·25221026	0·56795480E − 01	0·18014832E − 01	0·71601627E − 02	0·47596153
3·0000008	0·73013345	97·504019	2·1402793	0·26680240	0·61356267E − 01	0·19688234E − 01	0·78551597E − 02	0·72519444
3·5000948	0·89416403	97·340662	2·2631985	0·29533098	0·69312347E − 01	0·22487656E − 01	0·90084398E − 02	0·89305168
4·0000531	1·0277860	97·093824	2·4545770	0·33470422	0·80081683E − 01	0·26251769E − 01	0·10561071E − 01	1·0296949
4·5000782	1·1460710	96·786903	2·6934397	0·38295271	0·93324841E − 01	0·30895386E − 01	0·12484629E − 01	1·1508946
5·0000837	1·2556773	96·436886	2·9645567	0·43862045	0·10880702	0·36365833E − 01	0·14763821E − 01	1·2635974
−5·0000775	1·6189098	−97·764720	−1·8341847	−0·29127315	−0·74352563E − 01	−0·25220114E − 01	−0·10249358E − 01	1·6282238
−4·5000209	1·5735260	−98·345975	−1·3575139	−0·21558926	−0·54847656E − 01	−0·18560895E − 01	−0·75134217E − 02	1·5799216
−4·0000052	1·5383697	−98·942006	−0·86130116	−0·14261571	−0·36619718E − 01	−0·12437646E − 01	−0·50193448E − 02	1·5421786
−3·5000734	1·5163703	−99·558694	−0·34049695	−0·71820104E − 01	−0·19483399E − 01	−0·67742220E − 02	−0·27317532E − 02	1·5178525
−3·0000722	1·5117824	−99·776474	0·21660491	−0·18338702E − 02	−0·30615978E − 02	−0·14341186E − 02	−0·59178391E − 03	1·5110585
−2·5000607	1·5313089	−99·086509	0·82629658	0·68959129E − 01	0·13052094E − 01	0·37230449E − 02	0·14600117E − 02	1·5282043
−2·0000494	1·5867435	−98·266336	1·5452999	0·14575199	0·29989639E − 01	0·90546503E − 02	0·35679241E − 02	1·5804640
−1·5000593	1·7025648	−97·157226	2·5281512	0·24236504	0·50690737E − 01	0·15472900E − 01	0·60938164E − 02	1·6907222
−1·0000660	1·9442886	−95·195418	4·2846439	0·40047946	0·83772521E − 01	0·25611991E − 01	0·10074009E − 01	1·9186042
−0·80008291	2·1181989	−93·740751	5·5973602	0·51018036	0·10641367	0·32514160E − 01	0·12781103E − 01	2·0793940
−0·60008838	2·3924208	−91·202794	7·9053768	0·68834793	0·14279603	0·43570699E − 01	0·17114852E − 01	2·3258678
−0·40001078	2·9070751	−85·326414	13·329141	1·0407356	0·21334160	0·64902841E − 01	0·25464804E − 01	2·7563397
−0·30005862	3·4306551	−77·364293	20·841335	1·3938865	0·28163908	0·85385011E − 01	0·33461154E − 01	3·1290574
−0·25000802	3·9904127	−65·667535	32·175638	1·6827560	0·33384200	0·10078735	0·39442435E − 01	3·3981105

†*Note*: See footnote to Table 2.

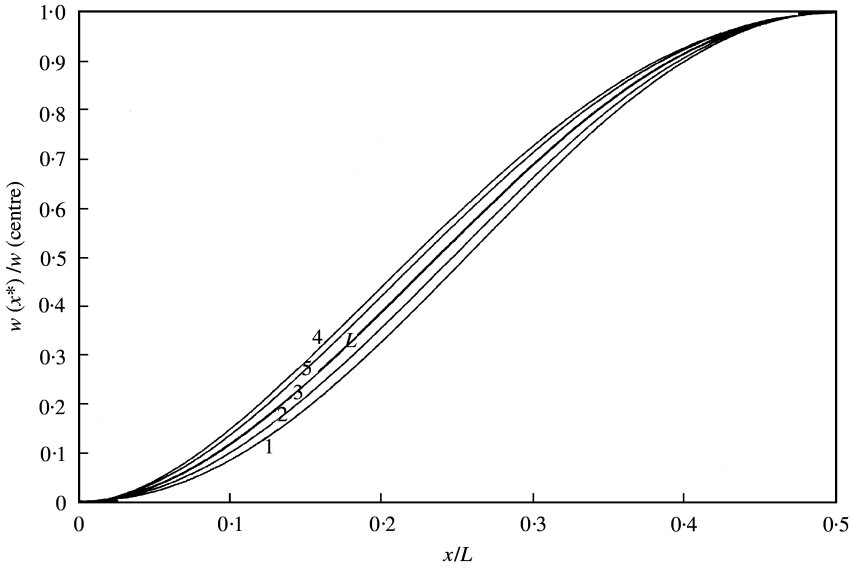

Figure 15. Linear and non-linear forced vibration deflection shapes of a fully clamped beam under a harmonic distributed force ($For^d = 1000$) at various amplitudes: *L*, Linear mode; 1, 2, 3, 4, 5, non-linear deflection corresponding to decreasing frequency from $\omega/\omega_L = 2$ to 1·1, ($\omega/\omega_L = 2$, w(centre)$/R = -0{\cdot}92696$); 2, ($\omega/\omega_L = 1{\cdot}7$, w(centre)$/R = -1{\cdot}50806$); 3, ($\omega/\omega_L = 1{\cdot}50996$, w(centre)$/R = -3{\cdot}17709$); 4, ($\omega/\omega_L = 1{\cdot}50665$, w(centre)$/R = 6{\cdot}22885$) and 5, ($\omega/\omega_L = 1$, w(centre)$/R = 3{\cdot}88990$).

beam at various amplitudes are presented in Figure 2. This figure clearly shows the influence of the non-linear effect especially at the centre and in the regions of the clamps.

4.1.3. *C–S beams*

For the analysis of a clamped–simply supported beam, the modal functions are given in Appendix A.3. The non-linear frequencies and the modal participations for various amplitudes using three symmetric and three antisymmetric modes are given in Table 6. In this case, due to the non-symmetry of the present problem, all symmetric and antisymmetric modes contribute to the solution. Comparison with published results of the non-linear frequencies and the axial forces for various amplitudes at the centre of the beam are presented in Table 7. These results show good agreement with those from previous works. In Table 8, the percentages of participation to the curvature of the first non-linear mode at the clamped end and at the centre of the beam are presented. This table clearly shows that the contributions of higher modes to the curvatures may be about 50% for a dimensionless amplitude at the centre of 10 and about 30% for a dimensionless amplitude of 5 (corresponding to w(centre)$/h = 1{\cdot}443$), which is very significant and cannot be neglected. The influence of the number of beam functions on the non-linear frequency estimates is presented in Table 9. It appears that for a C–S beam, the simple formula based on the single mode approach gives a good approximation of the non-linear frequency. The bending moments at the clamped end and at the centre of the beam obtained with various multi-dimensional models are presented in Table 10. As the difference between the results predicted by the various models is relatively higher, the multimodel analysis is necessary. The linear and non-linear mode shapes at various amplitudes, normalized by the displacement at the centre of the beam, are presented in Figure 3. The bending moments for

TABLE 13

Frequency ratios of non-linear forced vibrations of a C–C beam under a harmonic concentrated force at a quarter span of the beam using three symmetric and three antisymmetric modes and $For^C = 200$. *Modal participation and axial forces*

($For^C = 200$.D0). w(centre)/R	ω^*/ω_L^*	Modal participation (%)† a_1	a_2	a_3	a_4	a_5	a_6	NL^2/EI
1·0003	0·71789	86·103	10·557	2·6151	0·38717	−0·14099	−0·19618	2·6303
1·5002	0·86345	90·067	7·4445	2·0005	0·27741	−0·74802E − 01	−0·13576	5·6937
2·0001	0·95491	92·243	5·6394	1·7745	0·21852	−0·22341E − 01	−0·10231	9·9676
2·5004	1·0321	93·520	4·4445	1·7451	0·18162	0·28158E − 01	−0·80751E − 01	15·460
3·0000	1·1056	94·270	3·5915	1·8361	0·15615	0·80632E − 01	−0·65610E − 01	22·158
3·5000	1·1793	94·712	2·9513	2·0084	0·13726	0·13681	−0·54353E − 01	30·076
4·0001	1·2546	94·943	2·4548	2·2373	0·12245	0·19728	−0·45660E − 01	39·211
4·5001	1·3319	95·022	2·0609	2·5055	0·11033	0·26209	−0·38764E − 01	49·565
5·0004	1·4112	94·992	1·7430	2·8002	0·10005	0·33109	−0·33180E − 01	61·147
−5·0000	1·4855	−95·738	1·8180	−1·9223	0·10267	−0·38480	−0·33664E − 01	60·723
−4·5000	1·4193	−95·879	2·1634	−1·4800	0·11356	−0·32502	−0·39428E − 01	49·205
−4·0001	1·3586	−95·928	2·5978	−1·0292	0·12652	−0·27152	−0·46591E − 01	38·910
−3·5001	1·3048	−95·851	3·1555	−0·56970	0·14246	−0·22527	−0·55687E − 01	29·829
−3·0001	1·2597	−95·592	3·8919	−0·097859	0·16296	−0·18748	−0·67573E − 01	21·962
−2·5000	1·2260	−94·306	4·8676	0·39543	0·18942	−0·15853	−0·83104E − 01	15·306
−2·0001	1·2082	−92·318	6·2745	0·93250	0·22773	−0·14224	−0·10518	9·8654
−1·5000	1·2152	−89·308	8·5318	1·5864	0·28977	−0·14374	−0·13982	5·6363
−1·0000	1·2701	−83·824	12·826	2·5661	0·40648	−0·17554	−0·20262	2·6278
−0·80003	1·3205	−79·974	15·911	3·1793	0·48703	−0·20420	−0·24494	1·7696
−0·60007	1·4076	−73·906	20·859	4·0701	0·60769	−0·25019	−0·30731	1·1150
−0·40004	1·5795	−62·768	30·218	5·4844	0·79969	−0·32540	−0·40432	0·68601
−0·20004	2·0698	−34·662	56·275	7·1678	1·0031	−0·39844	−0·49365	0·78690

†*Note*: See footnote to Table 2.

TABLE 14

Bending moments and modal contributions at various amplitudes of forced vibration of a C–C beam under concentrated harmonic force at a quarter span ($For^c = 200$)

				Modal participation (%)†					
w(centre)/R	$\omega/\omega L$	$M^*(0)$	$M^*(1/2)$	$a_1v_1^2$	$a_2v_2^2$	$a_3v_3^2$	$a_4v_4^2$	$a_5v_5^2$	$a_6v_6^2$
0·70035	0·52251	33·989	−8·7148	54·288	25·372	12·218	3·0497	−1·7949	−3·2767
0·80014	0·60862	36·959	−10·407	57·282	23·772	11·436	2·8389	−1·6365	−3·0349
1·0002	0·71782	42·866	−13·794	62·240	21·039	10·217	2·5004	−1·3603	−2·6435
1·5000	0·86339	57·650	−22·202	70·690	16·109	8·4858	1·9452	−0·78375	−1·9862
2·0006	0·95500	72·826	−30·492	75·903	12·788	7·8898	1·6059	−0·24469	−1·5686
2·5004	1·0321	88·595	−38·596	78·784	10·321	7·9445	1·3667	0·31663	−1·2678
3·0000	1·1056	105·15	−46·497	80·035	8·4052	8·4238	1·1843	0·91348	−1·0382
3·5004	1·1794	122·67	−54·201	80·424	6·9068	9·2168	1·0411	1·5509	−0·86007
4·0002	1·2546	141·19	−61·680	80·203	5·7159	10·214	0·92403	2·2241	−0·71886
4·5002	1·3319	160·82	−68·960	79·551	4·7557	11·335	0·82505	2·9282	−0·60481
5·0001	1·4111	181·58	−76·050	78·598	3·9759	12·520	0·73955	3·6551	−0·51173
5·4999	1·4923	203·49	−82·978	77·444	3·3390	13·720	0·66458	4·3973	−0·43510
−5·5000	1·5562	−181·18	87·948	−79·692	3·5396	−10·614	0·69500	−5·0088	−0·45012
−5·0000	1·4855	−158·17	81·252	−81·260	4·2535	−8·8174	0·77842	−4·3584	−0·53252
−4·5000	1·4193	−136·30	74·390	−82·706	5·1442	−6·8992	0·87509	−3·7414	−0·63389
−4·0000	1·3586	−115·58	67·335	−83·947	6·2667	−4·8669	0·98903	−3·1706	−0·75992
−3·5000	1·3048	−95·987	60·064	−84·866	7·7016	−2·7254	1·1267	−2·6614	−0·91897
−3·0000	1·2596	−77·481	52·565	−85·300	9·5735	−0·47153	1·2990	−2·2323	−1·1239
−2·5000	1·2260	−59·981	44·832	−81·851	11·645	1·8545	1·4686	−1·8361	−1·3443
−2·0000	1·2082	−43·384	36·878	−76·583	14·348	4·1805	1·6876	−1·5746	−1·6263
−1·5000	1·2152	−27·522	28·723	−69·495	18·300	6·6706	2·0142	−1·4925	−2·0277
−1·0001	1·2701	−12·118	20·407	−58·704	24·758	9·7106	2·5428	−1·6404	−2·6446
−0·80002	1·3205	−5·9423	17·049	−52·389	28·731	11·255	2·8500	−1·7850	−2·9905
−0·60007	1·4076	0·42428	13·686	−44·019	34·247	13·100	3·2333	−1·9885	−3·4115
−0·40004	1·5795	7·5403	10·339	−32·234	42·777	15·220	3·6686	−2·2299	−3·8700
−0·30000	1·7458	12·182	8·6964	−24·225	49·564	16·085	3·8166	−2·3042	−4·0046

†*Note*: See footnote to Table 3.

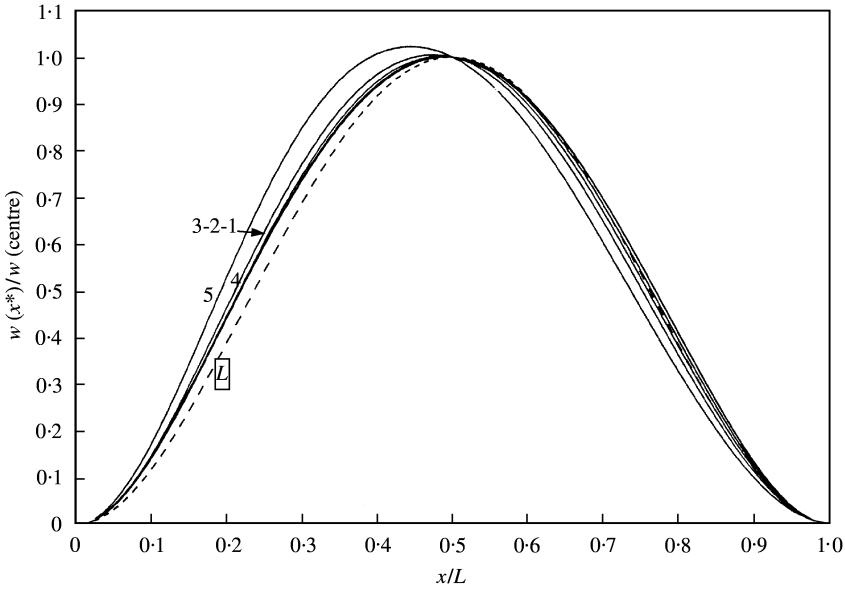

Figure 16. Linear and non-linear forced vibration deflection shapes of a fully clamped beam under a harmonic concentrated force at $L/4$ at positive amplitudes. ($For^C = 200$: L, linear mode; $1, 2, 3, 4, 5$, correspond to the numerical results given in Table 13 for $w(\text{centre})/R = 1, 2, 3, 4$ and 5 respectively.

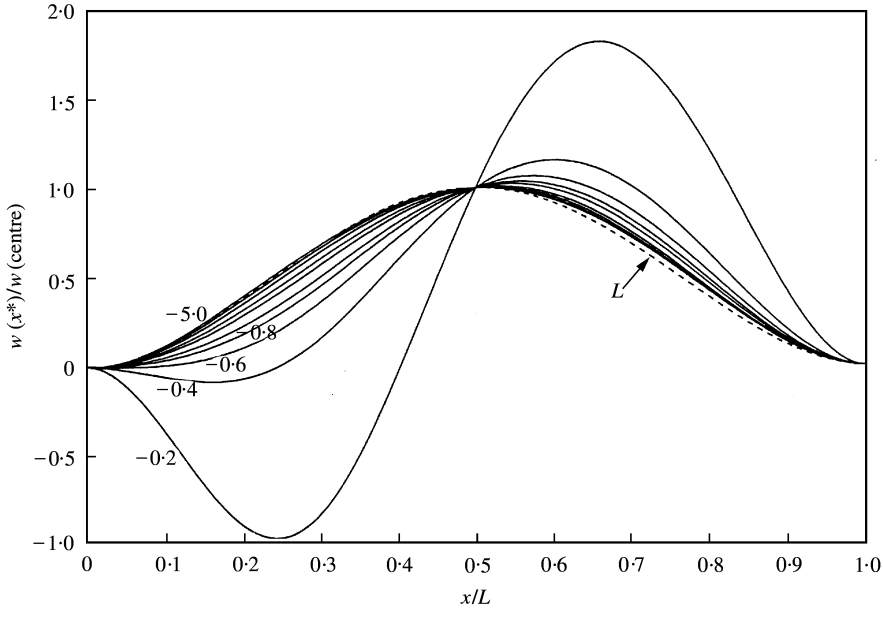

Figure 17. Linear and non-linear forced vibration deflection shapes of a fully clamped beam under a harmonic concentrated force at $L/4$ at negative amplitudes. ($For^C = 200$: L, linear mode, the other curves correspond to the numerical results given in Table 13 for $w(\text{centre})/R$ variant from -5 to $-0{\cdot}2$.

values of $w(\text{centre})/R$ of 1, 3, 5, 7 and 10 are given in Figure 4. For the second non-linear mode, the linear and non-linear mode shapes and the bending moments at various amplitudes at a quarter of the beam are presented in Figures 5 and 6. These figures clearly show the influence of the non-linearity on the displacements and the bending

TABLE 15

Frequency ratios of non-linear forced vibrations of a C–S beam under a harmonic concentrated force at a quarter span of the beam using three symmetric and three antisymmetric modes and $For^C = 200$. *Modal participation and axial forces*

		Modal participation (%)†						
w(centre)/R	ω^*/ω_L^*	a_1	a_2	a_3	a_4	a_5	a_6	NL^2/EI
0·80005	0·19540	79·172	15·762	3·9708	0·77078	−0·96319E − 01	−0·22744	1·6201
1·0004	0·52536	82·421	13·346	3·3222	0·64843	−0·75528E − 01	−0·18639	2·5091
2.0001	0·97679	89·547	7·9770	1·9636	0·41548	−0·10699E − 01	−0·85862E − 01	10·183
3·0000	1·2426	91·254	6·6199	1·6490	0·39946	0·44132E − 01	−0·33729E − 01	23·106
3·5000	1·3695	91·360	6·4936	1·6364	0·42480	0·73535E − 01	−0·11909E − 01	31·457
4·0001	1·4964	91·191	6·5538	1·6776	0·46404	0·10487	0·91129E − 02	41·035
4·5000	1·6239	90·835	6·7274	1·7554	0·51364	0·13815	0·29983E − 01	51·822
5·0000	1·7521	90·378	6·9685	1·8584	0·57115	0·17332	0·51075E − 01	63·810
−5·0004	1·8717	−95·099	−3·4788	−0·77616	−0·32785	−0·19628	−0·12202	65·721
−4·5003	1·7631	−96·544	−2·4634	−0·47975	−0·23404	−0·16646	−0·11210	53·860
−4·0000	1·6602	−98·176	−1·2820	−0·15806	−0·13917	−0·13983	−0·10513	43·162
−3·5000	1·5648	−99·433	0·11208	0·19581	−0·041909	−0·11632	−0·10124	33·635
−3·0000	1·4794	−97·456	1·7203	0·57373	0·056965	−0·094178	−0·98643	25·269
−2·5000	1·4081	−95·096	3·5805	0·98729	0·15636	−0·078210	−0·10160	18·070
−2·0000	1·3574	−92·223	5·8591	1·4725	0·26318	−0·069422	−0·11230	12·053
−1·549499	1·3391938	−88·8000	8·58425	2·03621	0·379123	−0·0692023	−0·132199	7·66795
−1·549398	1·3391938	−88·7991	8·58498	2·03636	0·378152	−0·0692032	−0·132205	7·66707
−1·5000	1·3395	−88·344	8·9474	2·1104	0·39276	−0·069739	−0·13525	7·2468
−1·0001	1·3828	−82·093	13·9458	3·1109	0·58389	−0·084115	−0·18183	3·69429
−0·80008	1·4337	−78·090	17·169	3·7314	0·69899	−0·096554	−0·21334	2·6381
−0·60000	1·5228	−72·251	21·919	4·5988	0·85734	−0·11551	−0·25832	1·8025
−0·40002	1·6873	−62·830	29·744	5·8733	1·0849	−0·14411	−0·32393	1·2121
−0·30008	1·8254	−55·620	35·912	6·7098	1·2296	−0·16235	−0·36538	1·0334
−0·20000	2·0335	−45·652	44·801	7·5892	1·3736	−0·17970	−0·40521	0·98348

†*Note*: See footnote to Table 2.

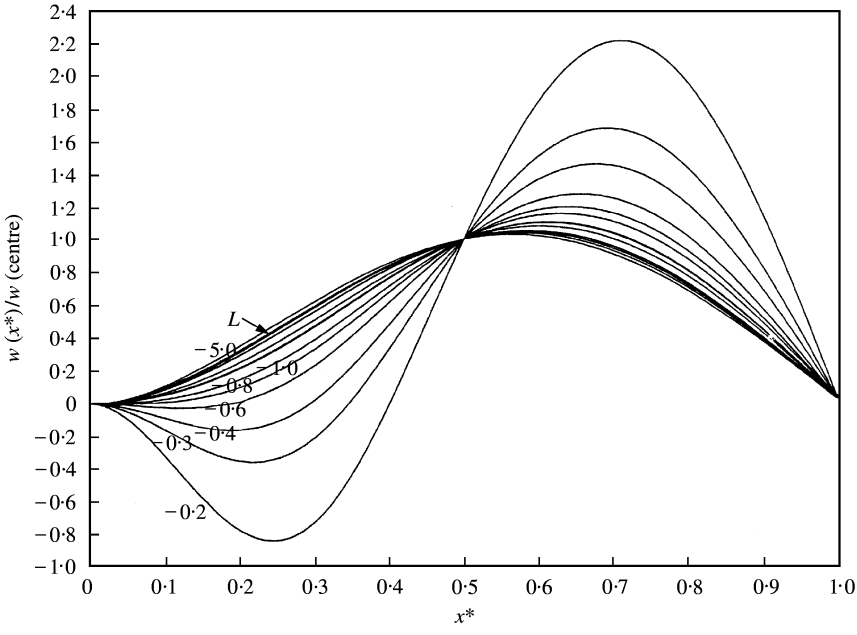

Figure 18. Linear and non-linear forced vibration deflection shapes of a clamped–simply supported beam under a harmonic concentrated force at $L/4$ at negative amplitudes. ($For^C = 200$: L, linear mode, the other curves correspond to the numerical results given in Table 15 for w(centre)$/R$ variant from -5 to $-0{\cdot}2$.

moments at large vibration amplitudes and that the effects are more pronounced at the clamped end.

4.2. FORCED VIBRATION

The numerical solution of equation (19) has been carried out with the forces given by equation (18). This permitted analysis of the effects of distributed forces and concentrated forces on the non-linear frequency and the non-linear response. For a C–C beam, six symmetric modes have been used for the analysis in the case of symmetric excitation. For a concentrated force acting at the centre of the beam ($For^c = 200$), the corresponding numerical results are presented in Table 11. A comparison is made with the single mode results and the contributions of higher modes are examined. It can be seen from these results that the influence of various modes is not negligible except in the vicinity of the limit of frequency which corresponds theoretically to the jump zone. This result is observed for positive and for "negative" amplitudes. The linear and non-linear resonance curves corresponding to a harmonic concentrated force at the centre of the C–C beam, ($For^c = 200$), are presented in Figure 7. These curves clearly show that the linear prediction leads to incorrect results for large vibration amplitudes. The linear and non-linear deflection shapes of the C–C beam at various zones of the frequency–amplitude curves are presented in Figure 8. The curve "a" corresponds to the zone, $0 < \omega/\omega_L < 1$, 'b' and 'c' correspond to the jump zone and 'd' and 'e' correspond to negative amplitudes, $1{\cdot}5 < \omega/\omega_L < 2$. For curve 'e', the influence of the second mode can be seen which can be also noted via the numerical results presented in Table 11. When the frequency tends to the second resonant frequency, the contribution of the second mode increases rapidly. The incremental procedure of the

contribution of the second mode will permit determination of the second frequency response curve. The first frequency response curves corresponding to various amplitudes of the excitation ($For^c = 200$ and 500) are presented in Figure 9. A non-linear frequency response curve, corresponding to large frequency ranges and involving the first, second and third resonances corresponding to a harmonic concentrated force at the centre of a C–C beam are given in Figure 10. These curves were obtained using the iterative–incremental procedure presented in Appendix B for solving the non-linear algebraic model (19). The corresponding contributions of the higher modes are presented in Figures 11–14. All these curves represent a vectorial non-linear frequency response function $A(\omega)$, in which $A^t = \{a_1, a_2, \ldots, a_n\}$ is the vector defining the contributions of the basic functions to the non-linear response for a given frequency and given values of the excitation force.

The numerical results corresponding to a harmonic distributed force ($For^d = 1000$), the comparison with the single mode approach and the contribution in various modes are presented in Table 12. The linear mode and the non-linear responses in various frequency regions are presented in Figure 15. The case of a decreasing frequency from $\omega/\omega_L^1 = 2$ to 1 is chosen because it presented a numerical snap-through at $\omega/\omega_L^1 = 1{\cdot}5099$. This jump phenomenon may be seen in Figure 15 in the curves numbered 3 and 4. Curve number 3 coincides with the linear mode and curve 4 is associated with a higher amplitude.

For the case of a harmonic concentrated force at a quarter span of the C–C beam ($For^c = 200$), all symmetric and antisymmetric modes contribute significantly to the solution, as may be expected, due to the excitation position. The numerical results for the frequency ratios, axial forces and the contributions of the modes are presented in Table 13. These contributions are greater than those obtained for symmetric excitations. The bending moment at the clamped end and at the centre and the modal contributions are presented in Table 14. The linear and the non-linear deflection shapes corresponding to several positive amplitudes are presented in Figure 16. A significant difference can be observed between the linear mode and the non-linear responses at large amplitudes. For negative amplitudes, the non-linear response corresponding to the numerical results of Table 13 are given in Figure 17. This clearly shows the evolution of the deformation of the beam with increasing frequency.

The numerical results for a clamped–simply supported beam excited by a harmonic concentrated force at a quarter span (L/4) are presented in Table 15. The response curves corresponding to various negative amplitudes are presented in Figure 18. The evolution of the deformation of the beam from the first to the second resonance is clearly shown in Figures 17 and 18. For small amplitudes, the influence of the second mode is more pronounced and the beam tends to vibrate following the second resonance.

The displacement at the beam centre can be predicted by the single mode analysis as shown in Figure 7, but the non-linear responses of the whole of the beam and the bending moments cannot be obtained with significant accuracy.

5. CONCLUSIONS

The semi-analytical approach to the non-linear dynamic response of beams based on multi-mode analysis has been developed. The applicability of this method to the non-linear forced vibration of beams with various types of excitations and boundary conditions is established. This enabled the non-linear effect to be taken into account and the contributions of higher modes to be established. Various types of excitations such as harmonic distributed and concentrated forces have been considered. The cases of simply

supported, clamped–clamped and clamped–simply-supported boundary conditions have been investigated. Using the harmonic balance method, the dynamic equation of motion can be converted into a set of non-linear algebraic equations. Numerical solution using a continuation method enabled a vectorial non-linear frequency response function to be obtained as a solution of the multi-dimensional Duffing equation. The validity of the present formulation has been established through comparison of the present results with existing alternative solutions. The non-linear frequencies and response curves in various regions of the solution have been obtained for various types of excitations and boundary conditions. The axial forces and the bending moments are presented and may be useful in predicting the fatigue life of a beam subjected to a large amplitude vibration.

The present formulation and solution is general and simple. It provides a useful tool for studying the non-linear forced vibration of structures. The method can be readily applied in the study of the large amplitude vibration of plates and shells. Extensions can be made to include more effects of interest such as structural damping.

ACKNOWLEDGMENTS

The first author is grateful to Professor M. Potier-Ferry at University of Metz for the financial support and the opportunity to use the facilities in his laboratory. This paper was partially written while the first author enjoyed the hospitality of the "Laboratoire de Physique et Mécanique des Matériaux" at the University of Metz in France.

REFERENCES

1. L. Azrar, R. Benamar and R. G. White 1999 *Journal of Sound and Vibration* **224**, 183–207. A semi-analytical approach to the nonlinear dynamic response problem of S–S and C–C beams at large vibration amplitudes. Part I: general theory and application to the single mode approach to free and forced vibration analysis.
2. R. Benamar 1990 *Ph.D. Thesis*, *University of Southampton*. Nonlinear dynamic behaviour of fully clamped beams and rectangular isotropic and laminated plates.
3. R. Benamar, M. M. K. Bennouna and R. G. White 1989 *Proceedings of the Seventh International Modal Analysis Conference*, *Las Vegas*, *NV*, *U.S.A.* Nonlinear mode shapes and resonance frequencies of fully clamped beams and plates.
4. R. Benamar, M. M. K. Bennouna and R. G. White 1990 *Proceedings of the Eighth International Modal Analysis Conference*, Orlando, FL, U.S.A. Harmonic distortion of the nonlinear response of fully clamped beams and plates.
5. R. Benamar, M. M. K. Bennouna and R. G. White 1991 *Journal of Sound and Vibration* **149**, 179–195. The effects of large vibration amplitudes on the mode shapes and natural frequencies of thin elastic structures. Part I: simply supported and clamped–clamped beams.
6. R. Benamar, M. M. K. Bennouna and R. G. White 1993 *Journal of Sound and Vibration* **164**, 399–424. The effects of large vibration amplitudes on the mode shapes and natural frequencies of thin elastic structures. Part II: fully clamped rectangular isotropic plates.
7. R. Benamar, M. M. K. Bennouna and R. G. White 1994 *Journal of Sound and Vibration* **175**, 377–395. The effects of large vibration amplitudes on the mode shapes and natural frequencies of thin elastic structures. Part III: fully clamped rectangular isotropic plates-measurements of the mode shape amplitude dependence and spatial distribution of harmonic distortion.
8. L. Azrar and R. Benamar 1995 *5ème Colloque Maghrébin sur les Modèles Numériques de l'Ingénieur*, *E.M.I.*, *Rabat*, *Maroc*, Vol. II, 594–599. Etude des vibrations non linéaires forcées des poutres par une méthode semi-analytique.
9. C. S. Hsu 1960 *Quarterly of Applied Mathematics* **17,** 393–407. On the application of elliptic functions in nonlinear forced oscillations.
10. J. G. Eisley 1964 *Zeitschrift für Angewandte Mathematik und Physik* **15**, 167–175. Nonlinear vibration of beams and rectangular plates.

11. A. V. SRINIVASAN 1966 *International Journal of Nonlinear Mechanics* **1**, 179–191. Nonlinear vibrations of beams and plates.
12. D. A. EVENSEN 1968 *American Institute of Aeronautics and Astronautics Journal* **6**, 370–372. Nonlinear vibrations of beams with various boundary conditions.
13. M. M. K. BENNOUNA and R. G. WHITE 1984 *Journal of Sound and Vibration* **96**, 309–331. The effects of large vibration amplitudes on the fundamental mode shape of a clamped–clamped uniform beam.
14. P. C. DUMIR and A. BHASKAR 1988 *Journal of Sound and Vibration* **123**, 517–527. Some erroneous finite element formulations of nonlinear vibrations of beams and plates.
15. M. I. QAISI 1993 *Applied Acoustics* **40**, 141–151. Application of the harmonic balance principle to the nonlinear free vibration of beams.
16. G. SINGH, A. K. SHARMA and G. VENKATESWARA RAO 1990 *Journal of Sound and Vibration* **142**, 77–85. Large amplitude free vibrations of beams. A discussion on various formulations and assumptions.
17. J. A. BENNETT and J. G. EISLEY 1970 *American Institute of Aeronautics and Astronautics Journal* **8**, 734–739. A multiple degree of freedom approach to nonlinear beam vibrations.
18. H. R. BUSBY J. and V. I. WEINGARTEN 1972 *International Journal of Nonlinear Mechanics* **7**, 289–303. Nonlinear response of a beam to periodic loading.
19. R. LEWANDOWSKI 1987 *Journal of Sound and Vibration* **114**, 91–101. Application of the Ritz method to the analysis of nonlinear free vibrations of beams.
20. C. MEI 1973 *Computers and Structures* **3**, 163–174. Finite element displacement method for large amplitude free flexural vibrations of beams and plates.
21. C. MEI and K. DECHA-UMPHAI 1985 *Journal of Sound and Vibration* **102**, 369–380. A finite element method for nonlinear forced vibrations of beams.
22. C. MEI and K. DECHA-UMPHAI 1985 *American Institute of Aeronautics and Astronautics Journal* **23**, 1104–1110. Finite element method for nonlinear forced vibration of rectangular plates.
23. G. VENKATESWARA RAO, K. KANAKA RAJU and I. S. RAJU 1976 *Computers and Structures* **6**, 169–172. Finite element formulation for large amplitude free vibration of beams and orthotropic circular plates.
24. B. S. SARMA and T. K. VARADAN 1983 *Journal of Sound and Vibration* **86**, 61–70. Lagrange-type formulation for finite element analysis of nonlinear beam vibrations.
25. B. NAGESWARA RAO 1992 *Journal of Sound and Vibration* **155**, 523–527. Large amplitude free vibrations of simply supported uniform beams with immovable ends.
26. S. R. R. PILLAI and B. NAGESWARA RAO 1992 *Journal of Sound and Vibration* **159**, 527–531. On nonlinear free vibrations of simply supported uniform beams.
27. G. SINGH, G. VENKATESWARA RAO and N. G. R. IYENGAR 1990 *Journal of Sound and Vibration* **143**, 351–355. Re-investigation of large-amplitude free vibrations of beams using finite elements.
28. Y. K. CHEUNG and S. L. LAU 1982 *Earthquake Engineering and Structural Dynamics* **10**, 239–253. Incremental time–space finite strip method for non-linear structural vibrations.
29. A. Y. T. LEUNG 1989 *Computational Mechanics* **5**, 73–80. Nonlinear natural vibration analysis of beams by selective coefficient increment.
30. R. LEWANDOWSKI 1994 *Journal of Sound and Vibration* **170**, 577–593. Nonlinear free vibrations of beams by the finite element and continuation methods.
31. L. AZRAR, C. COCHELIN, N. DAMIL and M. POTIER-FERRY 1998 *Structural Dynamic Systems, Computational Techniques and Optimization, Computer-Aided Design and Engineering. Gordon-Breach International Series in Engineering, Technology and Applied Science*, Vol. 7, 103–141. As asymptotic-numerical method for nonlinear vibrations of elastic structures.
32. L. AZRAR, R. BENAMAR and M. POTIER-FERRY 1999 *Journal of Sound and Vibration* **220**, 695–727. An asymptotic numerical method for large amplitude free vibrations of thin elastic plates.
33. A. K. NOOR, C. M. ANDERSEN and J. M. PETERS 1993 *Computer Methods in Applied Mechanics and Engineering* **103**, 175–186. Reduced basis technique for nonlinear vibration analysis of composite panels.
34. A. H. NAYFEH and S. A. NAYFEH 1994 *Journal of Vibration and Acoustics* **116**, 129–136. On nonlinear modes of continuous systems.
35. Y. SHI and C. MEI 1996 *Journal of Sound and Vibration* **193**, 453–464. A finite element time domain modal formulation for large amplitude free vibrations of beams and plates.
36. Y. SHI, R. Y. Y. LEE and C. MEI 1997 *American Institute of Aeronautics and Astronautics Journal* **35**, 159–166. Finite element method for nonlinear free vibrations of composite plates.

37. H. F. WOLFE 1995 *Ph.D. Thesis, University of Southampton.* An experimental investigation of nonlinear behaviour of beams and plates excited to high levels of dynamic response.
38. R. R. CHEN, C. MEI and H. F. WOLFE 1996 *Journal of Sound and Vibration* **195**, 719–737. Comparison of finite element nonlinear beam random response with experimental results.
39. E. RIKS 1979 *International Journal of Solid and Structures* **15**, 529–551. An incremental approach to the solution of snapping and buckling problems.
40. E. RIKS 1984 *Computer Methods in Applied Mechanics and Engineering* **47**, 219–259. Some computational aspects of the stability analysis of nonlinear structures.
41. J. L. BATOZ and G. DHATT 1979 *International Journal of Numerical Methods in Engineering* **14**, 1262–1267. Incremental displacement algorithms for non linear problems.
42. J. L. BATOZ, G. DHATT and M. FAFARD 1985 *Actes du troisième Colloque de tendances actuelles en calcul des structures, Bastia*, 6–8 November, 129–143. Algorithmes de calcul automatique des configurations pré et post-flambement des structures.
43. M. A. CRISFIELD 1983 *International Journal for Numerical Methods and Engineering* **19**, 1269–1289. An arc-length method including line searchers and accelerations.
44. M. A. CRISFIELD 1991 Nonlinear finite element analysis of solid structures, Vol. 1, Essentials. New York: John Wiley.
45. W. WAGNER and P. WRIGGERS 1988 *Engineering and Computation* **5**, 103–109. A simple method for the calculation of post-critical branches.
46. E. CARRERA 1994 *Computer and Structures* **50**, 217–229. A study on arc-length-type methods and their operation failures illustrated by a simple model.
47. R. LEWANDOWSKI 1997 *International Journal of Solid and Structures* **34**, 1925–1947. Computational formulation of periodic vibration of geometrically non-linear structures. Part 1: theoretical background.
48. R. LEWANDOWSKI 1997 *International Journal of Solid and Structures* **34**, 1949–1964. Computational formulation of periodic vibration of geometrically non-linear structures. Part 2: numerical strategy and examples.
49. P. RIBEIRO and M. PETYT 1999 *Journal of Sound and Vibration* **224**, 591–624. Non-linear vibration of beams with internal resonance by hierarchical finite element method.

APPENDIX A

A.1. SIMPLY SUPPORTED BEAMS

The linear mode shapes of a simply supported beam are given by

$$w_i(x) = R\sin(\mathrm{i}\pi x/L) = R\sin(\mathrm{i}\pi x^*) = Rw_i^*(x^*).$$

Using equation (8) easily gives:

$$m_{ij}^* = \delta_{ij}/2, \qquad \delta_{ij} \text{ Kronecker's symbol},$$

$$k_{ij}^* = i^2j^2\pi^4\delta_{ij}/2, \qquad b_{ijkl}^* = ijkl\pi^4\delta_{ij}\delta_{kl}/4,$$

A.2. CLAMPED–CLAMPED BEAMS

The chosen basic functions $w_i(x)$ for a clamped–clamped beam are

$$w_i(x) = \frac{ch(v_i x/L) - \cos(v_i x/L)}{ch(v_i) - \cos(v_i)} - \frac{sh(v_i x/L) - \sin(v_i x/L)}{sh(v_i) - \sin(v_i)}. \tag{A.1}$$

The functions $w_i(x)$ were normalized in such manner that $m_{ij}^* = \int_0^1 w_i^*(x)w_j^*(x)\,\mathrm{d}x = \delta_{ij}$. The constants v_i obtained by numerically solving the equation $ch(v_i)\cos(v_i) = 1$ are as follows:

C–C Symmetric	C–C Asymmetric
$v_1 = 4{\cdot}730040744862704D0$	$v_2 = 0{\cdot}7853204624095838D + 01$
$v_3 = 10{\cdot}99560783800167D0$	$v_4 = 0{\cdot}14137165491257460D + 02$
$v_5 = 17{\cdot}27875965739948D0$	$v_6 = 0{\cdot}20420352245626060D + 02$
$v_7 = 23{\cdot}56194490204046D0$	$v_8 = 0{\cdot}26703537555508190D + 02$
$v_9 = 29{\cdot}84513020910325D0$	$v_{10} = 0{\cdot}32986722862692820D + 02$
$v_{11} = 36{\cdot}12831551628262D0$	$v_{12} = 0{\cdot}39269908169872415D + 02$

The coefficients of the 1-D NFRF in the case of C–C are given numerically by

$$k_{11}^* = 500{\cdot}5639,\ b_{1111}^* = 37{\cdot}83861,\ w_1^*(1/2) = 1{\cdot}588146262.$$

A.3. CLAMPED–SIMPLY SUPPORTED

The chosen basic functions $w_i(x)$ for clamped–simply supported beams are also given by equation (A.1). The constants v_i for C–S beam obtained by numerically solving the equation $tg(v_i) - th(v_i) = 0$ are as follows:

C–S Odd modes	C–S Even modes
$v_1 = 3{\cdot}926602312047919D0$	$v_2 = 7{\cdot}068582745628732d0$
$v_3 = 10{\cdot}21017612281303D0$	$v_4 = 13{\cdot}3517687777540d0$
$v_5 = 16{\cdot}49336143134641D0$	$v_6 = 19{\cdot}63495408493621D0$

In this case $k_{11}^* = 237{\cdot}72107$, $b_{1111}^* = 33{\cdot}134588$, $w_1^*(1/2) = 1{\cdot}44485645$.

APPENDIX B: ALGORITHMS

The algorithms presented here were used for solving problem (24) in which the unknowns are the frequency parameter ω and the vector $A = {}^t\{a_1, a_2, \ldots, a_n\}$. These algorithms will permit all the resonance curves to be determined automatically. In order to obtain the desired resonance curves, ω_0 can be chosen in the vicinity of a linear frequency.

B.1. STRATEGIES USED FOR SOLUTION

Ires indicates the resonance number, ω_{Ires}^L the *Ires*th linear fundamental frequency, and n the number of the degree of freedom of the system. The algorithms ALGOR1, ALGOR2 and ALGOR3 will be given later.

Begin ALTERNATING-ALGORITHM
Set $A[\ ] = [0]$, $\omega = 0$, $Ires = 0$
Choose N_1, N_2, N_3, $\Delta\omega^2$, α, Δa_q
Repeat
  Set $Ires = Ires + 1$ and $j = 0$
  Repeat
    Set $j = j + 1$

Set $\omega^2 = \omega^2 + \Delta\omega^2$
Call routine ALGOR1(A, ω^2)
Return the vector $A[\ ] = (a_1, a_2, \ldots, a_n)$

Until ($j = N1$ or $\omega = \alpha(\omega^L_{(Ires+1)} - \omega^L_{Ires})$)
Set $A[\ ] = -A[\ ]$

Set $aq = a_{Ires}$, $k = 0$
Repeat
Set $k = k + 1$
Set $a_q = a_q + \Delta a_q$
Set $\omega_1 = \omega$
Call ALGOR2(A, ω^2, a_q, Δa_q)
Return $A[\ ]$ and ω^2
Until($k = N_2$) or ($\omega_1 < \omega$)
Until $Ires = n$

- or -

Repeat
Set $k = k + 1$
Call ALGOR3(A, ω^2, s)
Return $A[\ ]$ and ω^2
Until($k = N_3$)
Until $Ires = n$

For more detail and applicability of Newton–Raphson procedures, one can refer to the papers of Riks [39, 40], Batoz *et al.* [41, 42], Crisfield [43, 44] and Wagner *et al.* [45]. Various formulations and applications to some non-linear structural problems are also formulated by various authors [46–49].

B.2. ALGOR1: IMPOSED FREQUENCY

Begin ALGOR1(A, ω^2)
Choose ε, k_{max}
Set $k = 0$
Repeat
Set $k = k + 1$
If ($k = k_{max}$) then
Exit–No convergence-
Endif
Compute the residue $\mathbf{G}(\mathbf{A}, \omega^2)$
If ($\|\mathbf{G}(\mathbf{A}, \omega^2)\| < \varepsilon$) then
Return
Endif
Compute the tangent matrix $\mathbf{K}_t(\mathrm{A}, \omega^2)$
Solve linear system $\mathbf{K}_t \cdot \Delta\mathbf{A} = -\mathbf{G}(\mathbf{A}, \omega^2)$ for $\mathbf{A}[\ ]$
Set $\mathbf{A} = \mathbf{A} + \Delta\mathbf{A}$
Until $k = k_{max}$
Output $\mathbf{A}[\ ]$.

B.3. ALGOR2: IMPOSED DISPLACEMENT

Begin ALGOR2($\mathbf{A}$, ω^2, aq, Δaq)
choose ε, k_{max}
compute $\mathbf{K}_t(\mathbf{A}, \omega^2)$ and $\mathbf{G}_{,\omega^2} = \dfrac{\partial \mathbf{G}(\mathbf{A}, \omega)}{\partial \omega^2}$
solve $\mathbf{K}_t \cdot \Delta\mathbf{X} = -\mathbf{G}_{,\omega^2}$ for $\Delta\mathbf{X}[\ ]$

set $\Delta\omega^2 = \dfrac{\Delta a_q}{\Delta \mathbf{X}(q)}$
set $\mathbf{A} = \mathbf{A} + \Delta\omega^2 \Delta\mathbf{X}$ and $\omega^2 = \omega^2 + \Delta\omega^2$ prediction
set $k = 0$
repeat
  set $k = k + 1$
  If $(k = k_{max})$ then
    exit – no convergence –
  endif
  compute $\mathbf{K}_t(\mathbf{A}, \omega^2)$, $\mathbf{G}_{,\omega^2}$ and $\mathbf{G}(\mathbf{A}, \omega^2)$
  solve $\mathbf{K}_t \cdot \Delta\mathbf{X}_R = -\mathbf{G}(\mathbf{A}, \omega^2)$ and $\mathbf{K}_t \cdot \Delta\mathbf{X}_F = -\mathbf{G}_{,\omega^2}(\mathbf{A}, \omega^2)$
  set $\Delta\omega^2 = -\dfrac{\Delta\mathbf{X}_R(q)}{\Delta\mathbf{X}_F(q)}$
  set $\mathbf{A} = \mathbf{A} + \Delta\mathbf{X}_R + \Delta\omega^2\Delta\mathbf{X}_F$ and $\omega^2 = \omega^2 + \Delta\omega^2$ correction
  If $(\|\mathbf{G}(\mathbf{A}, \omega^2)\| < \varepsilon)$ then
    return
    endif
until $k = k_{max}$
output $\mathbf{A}[\ ]$ and ω^2.

B.4. ALGOR3: ARC-LENGTH METHOD

Choose ε, s and k_{max}
Begin ALGOR3(A, ω^2, s)
set $\mathbf{AP}[\ ] = \mathbf{A}[\ ]$
compute $\mathbf{K}_t$ and $\mathbf{G}_{,\omega^2}$
solve $\mathbf{K}_t \cdot \Delta\mathbf{X} = -\mathbf{G}_{,\omega^2}$
set $\Delta\omega^2 = \dfrac{s}{\sqrt{\langle \Delta\mathbf{X}, \Delta\mathbf{X}\rangle}}$
set $\mathbf{A} = \mathbf{A} + \Delta\omega^2\Delta\mathbf{X}$ and $\omega^2 = \omega^2 + \Delta\omega^2$ prediction
$k = 0$
repeat
  set $k = k + 1$
  If $(k = k_{max})$ then
    exit–no convergence–
  endif
  compute $\mathbf{K}_t(\mathbf{A}, \omega^2)$, $\mathbf{G}_{,\omega^2}(\mathbf{A}, \omega^2)$ and $\mathbf{G}(\mathbf{A}, \omega^2)$
  solve $\mathbf{K}_t \cdot \Delta\mathbf{X}_R = -\mathbf{G}$
  solve $\mathbf{K}_t \cdot \Delta\mathbf{X}_F = -\mathbf{G}_{,\omega^2}$
  set $\mathbf{V} = \Delta\mathbf{X}_R + \mathbf{A} - \mathbf{AP}$
  Set $a = \langle \Delta\mathbf{X}_F, \Delta\mathbf{X}_F\rangle$, $b = 2\langle \Delta\mathbf{X}_F, \mathbf{V}\rangle$ and $c = \langle \mathbf{V}, \mathbf{V}\rangle - s^2$
  solve $a(\Delta\omega^2)^2 + b\Delta\omega^2 + c = 0$
  choose $\Delta\omega$ = absolute value of the smaller solution
  set $\mathbf{A} = \mathbf{A} + \Delta\mathbf{X}_R + \Delta\omega^2\Delta\mathbf{X}_F$, $\omega^2 = \omega^2 + \Delta\omega^2$ correction
  If $(\|\mathbf{G}(\mathbf{A}, \omega^2)\| < \varepsilon)$ then
    return
  endif

until $k = k_{max}$
output $\mathbf{A}[\ ]$ and ω^2.

APPENDIX C: NOMENCLATURE

$U(x, t)$, $W(x, t)$	axial and transverse displacements at point x on the beam
ε, K	axial strain, curvature
N, M	axial resultant force, bending moment
E, h	Young's modulus of a beam, the thickness of the beam
ρ	mass per unit length of the beam
L, S, I	length, area and second moment of area of cross-section of the beam
$W(x, t)$	transverse displacement at point x on the beam
V	stream energy
T	kinetic energy
q_i	generalized co-ordinate $q_i(t) = a_i \cos(wt)$
$w_i(x)$	the ith mode of the beam
$\{\mathbf{A}\}$	column matrix of basic function contributions to the forced response $\{\mathbf{A}\}^t = [a_1, \ldots, a_n]$
ω_L	the linear natural frequency corresponding to the one mode assumed
k_{ij}, m_{ij}, b_{ijkl}	general term of the rigidity tensor, the mass tensor and the non-linearity tensors
[**K**], [**M**], [**B**]	rigidity, mass and non-linearity matrix respectively
k^*_{ij}, m^*_{ij}, b^*_{ijkl}	non-dimensional rigidity tensor, mass tensor and non-linearity tensor respectively
ω, $\omega/$	frequency and non-dimensional frequency parameter respectively
$F(x, t)$, Ω	exciting force, range of application of the exciting force
$\{\mathbf{F}(t)\}$	column matrix of generalized forces, $\{F(t)\} = \{f\}\cos(\omega t)$
R	the radius of gyration
F^d, F^c	the distributed force and the concentrated force at x_0
fi^{c*}, fi^{d*}	dimensionless concentrated and distributed forces
For^c, For^d	forcing coefficients
$\mathbf{K}_T$	tangent matrix at a known solution ($^1\mathbf{A}$, $^1\omega^*$)